

**N<sub>2</sub>O<sub>5</sub> uptake onto saline mineral dust: a potential missing source of tropospheric  
ClNO<sub>2</sub> in inland China**

Haichao Wang<sup>1,7,#</sup>, Chao Peng<sup>2,#</sup>, Xuan Wang<sup>3,#</sup>, Shengrong Lou<sup>4</sup>, Keding Lu<sup>5</sup>, Guicheng Gan<sup>6</sup>,  
Xiaohong Jia<sup>1</sup>, Xiaorui Chen<sup>5</sup>, Jun Chen<sup>6</sup>, Hongli Wang<sup>4</sup>, Shaojia Fan<sup>1,7</sup>, Xinming Wang,<sup>2,8,9</sup>  
Mingjin Tang<sup>2,8,9,\*</sup>

<sup>1</sup> School of Atmospheric Sciences, Sun Yat-sen University, Guangzhou, China

<sup>2</sup> State Key Laboratory of Organic Geochemistry, Guangdong Key Laboratory of Environmental  
Protection and Resources Utilization, and Guangdong-Hong Kong-Macao Joint Laboratory for  
Environmental Pollution and Control, Guangzhou Institute of Geochemistry, Chinese Academy of  
Sciences, Guangzhou, China

<sup>3</sup> School of Energy and Environment, City University of Hong Kong, Hong Kong SAR, China

<sup>4</sup> State Environmental Protection Key Laboratory of Formation and Prevention of the Urban Air  
Complex, Shanghai Academy of Environmental Sciences, Shanghai, China

<sup>5</sup> State Key Joint Laboratory of Environmental Simulation and Pollution Control, College of  
Environmental Sciences and Engineering, Peking University, Beijing, China

<sup>6</sup> Institute of Particle and Two-Phase Flow Measurement, College of Energy and Power  
Engineering, University of Shanghai for Science and Technology, Shanghai, China

<sup>7</sup> Guangdong Provincial Observation and Research Station for Climate Environment and Air  
Quality Change in the Pearl River Estuary, Key Laboratory of Tropical Atmosphere-Ocean System,  
Ministry of Education, Southern Marine Science and Engineering Guangdong Laboratory  
(Zhuhai), Zhuhai, China

24   <sup>8</sup> CAS Center for Excellence in Deep Earth Science, Guangzhou 510640, China

25   <sup>9</sup> University of Chinese Academy of Sciences, Beijing, China

26

27   <sup>#</sup>These authors contributed equally to this work

28   \*correspondence: Mingjin Tang ([mingjintang@gig.ac.cn](mailto:mingjintang@gig.ac.cn))

29

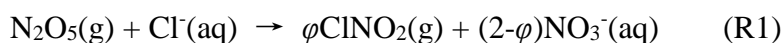
## Abstract

Nitryl chloride ( $\text{ClNO}_2$ ), an important precursor of Cl atoms, significantly affects atmospheric oxidation capacity and  $\text{O}_3$  formation. However, sources of  $\text{ClNO}_2$  in inland China have not been fully elucidated. In this work, laboratory experiments were conducted to investigate heterogeneous reaction of  $\text{N}_2\text{O}_5$  with eight saline mineral dust samples collected from different regions in China, and substantial formation of  $\text{ClNO}_2$  was observed.  $\text{ClNO}_2$  yields,  $\phi(\text{ClNO}_2)$ , showed large variations (ranging from  $<0.05$  to  $\sim 0.77$ ) for different saline mineral dust samples, largely depending on mass fractions of particulate chloride. In addition, for different saline mineral dust samples,  $\phi(\text{ClNO}_2)$  could increase, decrease or show insignificant change as RH increased from 18% to 75%. We further found that current parameterizations significantly overestimated  $\phi(\text{ClNO}_2)$  for heterogeneous uptake of  $\text{N}_2\text{O}_5$  onto saline mineral dust. In addition, assuming a uniform  $\phi(\text{ClNO}_2)$  value of 0.10 for  $\text{N}_2\text{O}_5$  uptake onto mineral dust, we used a 3-D chemical transport model to assess the impact of this reaction on tropospheric  $\text{ClNO}_2$  in China, and found that weekly mean nighttime maximum  $\text{ClNO}_2$  mixing ratios could be increased by up to 85 pptv during a severe dust event in May 2017. Overall, our work showed that heterogeneous reaction of  $\text{N}_2\text{O}_5$  with saline mineral dust could be an important source of tropospheric  $\text{ClNO}_2$  in inland China.

## 1 Introduction

The formation of O<sub>3</sub> and secondary aerosols, two major air pollutants, is closely related to atmospheric oxidation processes (Lu et al., 2019). Primary pollutants emitted by natural and anthropogenic sources are oxidized by various oxidants to produce O<sub>3</sub> and secondary aerosols, affecting air quality and climate. Major tropospheric oxidants include OH radicals, NO<sub>3</sub> radicals and O<sub>3</sub>, and in the last two decades Cl atoms have been proposed as an important oxidant (Saiz-Lopez and von Glasow, 2012; Simpson et al., 2015; Wang et al., 2019). Rate constants for reactions of certain volatile organic compounds (VOCs) with Cl atoms can be a few orders of magnitude larger than those reacting with OH radicals (Atkinson and Arey, 2003; Atkinson et al., 2006); therefore, despite its lower concentrations in the troposphere, Cl can contribute significantly to atmospheric oxidation capacity in some regions (Saiz-Lopez and von Glasow, 2012; Simpson et al., 2015; Wang et al., 2019). For example, a modeling study (Sarwar et al., 2014) suggested that including Cl chemistry in the model could enhance oxidative degradation of VOCs by >20% in some locations.

One major source of tropospheric Cl atoms is daytime photolysis of ClNO<sub>2</sub> (Thornton et al., 2010; Simpson et al., 2015), which is formed in heterogeneous reaction of N<sub>2</sub>O<sub>5</sub> with chlorine-containing particles (R1) at nighttime (Osthoff et al., 2008; Thornton et al., 2010):



The uptake coefficient,  $\gamma(\text{N}_2\text{O}_5)$ , and the ClNO<sub>2</sub> yield,  $\phi(\text{ClNO}_2)$ , both depend on relative humidity (RH), aerosol composition and mixing state, and etc. (Bertram and Thornton, 2009; Ryder et al., 2014; Mitroo et al., 2019; McNamara et al., 2020; Yu et al., 2020). Cl atoms produced by ClNO<sub>2</sub> photolysis can effectively enhance atmospheric oxidation (Le Breton et al., 2018; Wang et al., 2019) and thus increase concentrations of O<sub>3</sub> and OH radicals during the day (Simon et al., 2009;

Riedel et al., 2014; Sarwar et al., 2014; Tham et al., 2016; Wang et al., 2016). In addition, ClNO<sub>2</sub> is an important temporary reservoir of NO<sub>x</sub> at night and releases NO<sub>2</sub> during the daytime via photolysis, thereby further affecting daytime photochemistry.

Sea spray aerosol is the most important source of particulate chloride (Cl<sup>-</sup>), and ClNO<sub>2</sub> is expected to be abundant at marine and coastal regions impacted by anthropogenic emissions. High levels of ClNO<sub>2</sub> have been observed at various marine and coastal regions over the globe (Simon et al., 2009; Riedel et al., 2012; Tham et al., 2014; Young et al., 2014; Wang et al., 2016; Osthoff et al., 2018; Wang et al., 2020a; Yu et al., 2020). In addition, many studies (Thornton et al., 2010; Mielke et al., 2011; Phillips et al., 2012; Riedel et al., 2013; Bannan et al., 2015; Faxon et al., 2015; Wang et al., 2017b; Wang et al., 2017c; Tham et al., 2018; Wang et al., 2018) have also reported significant amounts of ClNO<sub>2</sub> at various continental sites with limited marine influence. For example, ClNO<sub>2</sub> concentrations reached 4 ppbv in the summer of North China Plain (Tham et al., 2016). These observations imply the importance of other sources for aerosol chloride, such as coal combustion (Eger et al., 2019), biomass burning (Ahern et al., 2017), waste incineration (Bannan et al., 2019), and snow-melting agent application (Mielke et al., 2016; McNamara et al., 2020).

In addition to insoluble minerals (e.g., quartz, feldspar, clay and carbonate), mineral dust aerosols emitted from saline topsoil in arid and semi-arid regions may contain significant amounts of soluble materials such as chloride and sulfate (Gillette et al., 1992; Abuduwailli et al., 2008; Zhang et al., 2009; Wang et al., 2012; Jordan et al., 2015; Frie et al., 2017; Gaston et al., 2017; Tang et al., 2019; Gaston, 2020). As elemental and mineralogical compositions are different for conventional and saline mineral dust, they would differ significantly in physicochemical properties and impacts on atmospheric chemistry and climate. For example, hygroscopicity and cloud condensation nuclei (CCN) activities of saline mineral dust can be much higher than conventional

mineral dust (Pratt et al., 2010; Gaston et al., 2017; Tang et al., 2019; Zhang et al., 2020). Recent laboratory studies (Mitroo et al., 2019; Royer et al., 2021) found that heterogeneous reactions of  $\text{N}_2\text{O}_5$  with saline mineral dust originating from western and southwestern USA can be very effective and produce significant amounts of  $\text{ClNO}_2$ . Large variations in  $\gamma(\text{N}_2\text{O}_5)$  and  $\phi(\text{ClNO}_2)$  were reported (Mitroo et al., 2019; Royer et al., 2021), depending on RH as well as chemical and mineralogical contents of saline mineral dust samples.

A very recent study (Wu et al., 2020) showed that  $\text{N}_2\text{O}_5$  uptake onto saline mineral dust contributed significantly to particulate nitrate formation during a dust storm event in Shanghai, China. One may further expect that it may have a profound effect on  $\text{ClNO}_2$ , especially considering that vast areas in China are heavily affected by both mineral dust and  $\text{NO}_x$ . Nevertheless, heterogeneous formation of  $\text{ClNO}_2$  from  $\text{N}_2\text{O}_5$  uptake onto saline mineral dust in other regions rather than USA has not been explored. In order to provide key parameters required to assess the potential of saline mineral dust as a  $\text{ClNO}_2$  source in China, we conducted a series of laboratory experiments to investigate  $\text{ClNO}_2$  formation in heterogeneous reaction of  $\text{N}_2\text{O}_5$  with several saline mineral dust samples collected from different regions in China. In addition to difference in source regions, saline mineral dust samples examined in our work have substantial variations in composition and mineralogy, enabling us to examine the effects of particle composition and water content on  $\text{ClNO}_2$  production. In order to better understand variations of  $\text{ClNO}_2$  yields with RH and samples, we experimentally measured mass hygroscopic growth factors of the eight samples examined, while previous studies (Mitroo et al., 2019; Royer et al., 2021) used the thermodynamic model ISORROPIA-II (Fountoukis and Nenes, 2007) to predict particulate water contents. Based on our laboratory results, we further use a 3-D chemical transport model (GEOS-Chem) to assess

the impacts of ClNO<sub>2</sub> produced from N<sub>2</sub>O<sub>5</sub> uptake onto mineral dust on ClNO<sub>2</sub> and O<sub>3</sub> in China during a major dust event which occurred in May 2017.

## 2 Methodology

### 2.1 Characterization of saline mineral dust samples

Eight saline mineral dust samples, originating from five different provinces in northern China (including Ningxia, Xinjiang, Shandong, Inner Mongolia and Shaanxi), were examined in this work, and full information of these samples can be found elsewhere (Tang et al., 2019). Table 1 summarizes key information of these samples. According to their chloride contents, the eight samples were classified into three categories, including two high chloride samples (H1 and H2), four medium chloride samples (M1, M2, M3 and M4) and two low chloride samples (L1 and L2).

Our previous work (Tang et al., 2019; Zhang et al., 2020) measured mass hygroscopic growth factors of the eight samples at 0-90% RH with a RH resolution of 10%, using a vapor sorption analyzer (Gu et al., 2017). As the highest RH at which heterogeneous reaction of N<sub>2</sub>O<sub>5</sub> with saline mineral dust was conducted in our work was ~75%, we further measured mass growth factors of the eight samples at (75±2)% RH, and the results are also included in Table 1.

**Table 1.** Overview of mass fractions of major soluble ions and mass ratios of particulate water at (75±2)% RH to dry particles for the eight saline mineral dust samples examined in this work. Mass fractions of major soluble ions were reported previously (Tang et al., 2019), and particulate water contents at (75±2)% RH were measured by the present work.

| category             | sample <sup>a</sup> | sample <sup>b</sup> | Na <sup>+</sup> | Cl <sup>-</sup> | SO <sub>4</sub> <sup>2-</sup> | H <sub>2</sub> O (75%) |
|----------------------|---------------------|---------------------|-----------------|-----------------|-------------------------------|------------------------|
| High Cl <sup>-</sup> | H1                  | NX                  | 0.3537          | 0.3870          | 0.0958                        | 1.3093                 |
|                      | H2                  | XJ-5                | 0.2407          | 0.2145          | 0.0973                        | 1.7066                 |

|                        |    |      |        |        |        |        |
|------------------------|----|------|--------|--------|--------|--------|
| Medium Cl <sup>-</sup> | M1 | SD   | 0.0265 | 0.0508 | 0.0754 | 0.3911 |
|                        | M2 | XJ-4 | 0.0326 | 0.0341 | 0.0071 | 0.0428 |
|                        | M3 | IM-2 | 0.0471 | 0.0229 | 0.1413 | 0.2106 |
|                        | M4 | IM-3 | 0.1343 | 0.0095 | 0.3424 | 0.0174 |
| Low Cl <sup>-</sup>    | L1 | XJ-3 | 0.0239 | 0.0093 | 0.0497 | 0.0475 |
|                        | L2 | SX   | 0.0003 | n.d.   | n.d.   | 0.0126 |

<sup>a</sup>: sample names used in the present work; <sup>b</sup>:corresponding sample names used in our previous work (Tang et al., 2019).

## 2.2 Experimental apparatus

Figure 1 shows the experimental apparatus used to study heterogeneous interactions of N<sub>2</sub>O<sub>5</sub> with saline mineral dust. It mainly consists of three parts: 1) N<sub>2</sub>O<sub>5</sub> generation, 2) gas-particle interaction, and 3) detection of N<sub>2</sub>O<sub>5</sub> and ClNO<sub>2</sub>.

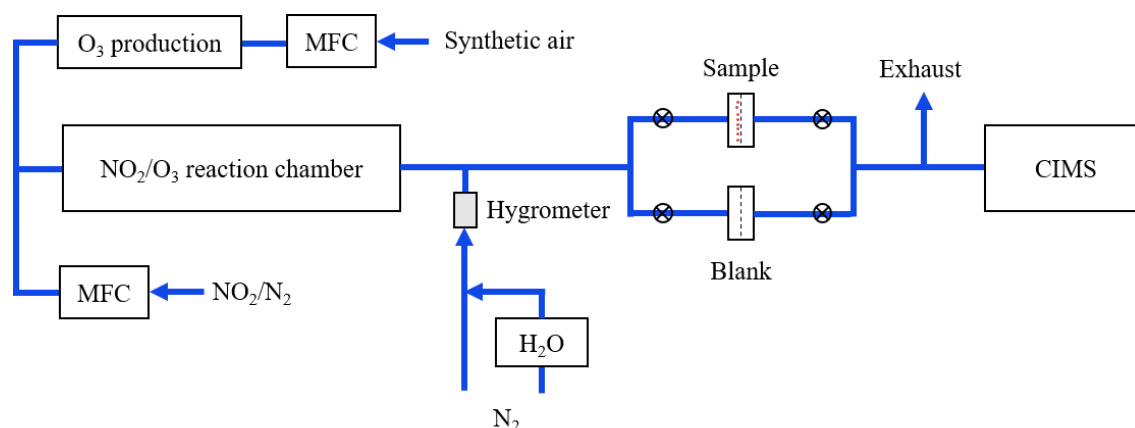


**Figure 1.** Schematic diagram of the experimental apparatus.

### 2.2.1 N<sub>2</sub>O<sub>5</sub> generation

In our work, N<sub>2</sub>O<sub>5</sub> was generated via oxidation of NO<sub>2</sub> by O<sub>3</sub>. As shown in Figure 1, a synthetic air flow (30 mL/min) was passed over a Hg lamp to produce O<sub>3</sub> via O<sub>2</sub> photolysis at 184.95 nm. The photolysis module was stabilized at 35±0.2 °C using a Peltier cooler controlled by a Proportion Integration Differentiation (PID) algorithm, in order to give stable O<sub>3</sub> output. The



O<sub>3</sub>/air flow was then mixed with a NO<sub>2</sub> flow (80 mL/min, 10 ppmv in synthetic air) in a temperature-stabilized PFA reactor with a residence time of ~70 s to produce N<sub>2</sub>O<sub>5</sub>. After exiting the PFA reactor, the flow (110 mL/min) was then diluted with a humidified nitrogen flow (2500 mL/min), and RH of the humidified nitrogen flow was monitored using a hygrometer. The final flow had a total flow rate of 2610 mL/min.

### 2.2.2 Heterogeneous interactions

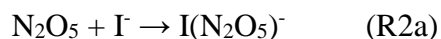
As shown in Figure 1, the mixed flow (2610 mL/min) could be directed through a blank PTFE membrane filter (47 mm, Whatman, USA) housed in a PFA filter holder, and in this case initial N<sub>2</sub>O<sub>5</sub> and ClNO<sub>2</sub> concentrations were measured; **in our experiments, initial N<sub>2</sub>O<sub>5</sub> concentrations were in the range of 0.4-1.0 ppbv.** Alternatively, the flow could also be passed through a PTFE filter loaded with saline mineral dust, and thus N<sub>2</sub>O<sub>5</sub> and ClNO<sub>2</sub> concentrations after heterogeneous reaction with saline mineral dust loaded on the filter were measured. During our experiments, the flow could be switched back to pass through the blank filter in order to check whether the initial N<sub>2</sub>O<sub>5</sub> and ClNO<sub>2</sub> concentrations were stable.

Saline mineral dust particles were loaded onto PTFE filters using the method described in our previous study (Li et al., 2020; Jia et al., 2021). **In brief, 10 mL particle/ethanol mixture was transferred onto a PTFE filter, and after ethanol was evaporated a relatively uniform particle film, as revealed by visual inspection, was formed on the filter.** PTFE filters were weighted before and after being loaded with particles, in order to determine the mass of particles loaded onto these filters. In our work, the mass of particles on filters were in range of 0.6-7.3 mg.

### 2.2.3 Detection of N<sub>2</sub>O<sub>5</sub> and ClNO<sub>2</sub>

After exiting one of the two filters, a flow of 2200 mL/min was sampled into a time-of-flight chemical ionization mass spectrometry (TOF-CIMS) to measure N<sub>2</sub>O<sub>5</sub> and ClNO<sub>2</sub> concentrations,

and the remaining flow (~400 mL/min) went into the exhaust. The CIMS instrument has been detailed previously (Kercher et al., 2009; Wang et al., 2016). In brief, N<sub>2</sub>O<sub>5</sub> and ClNO<sub>2</sub> were detected as I(N<sub>2</sub>O<sub>5</sub>)<sup>-</sup> and I(ClNO<sub>2</sub>)<sup>-</sup> clusters at 235 and 208 m/z (R2a, R2b) using I<sup>-</sup> as the reagent ion, and a soft X-ray device (Hamamatsu, Soft X-Ray 120°) was employed to generate I<sup>-</sup> from CH<sub>3</sub>I/N<sub>2</sub>. CIMS was calibrated before and after our experiments which lasted for ~1 month, and further details on calibration can be found in the Appendix. The detection limits were 2 pptv for N<sub>2</sub>O<sub>5</sub> and 3 pptv for ClNO<sub>2</sub>, calculated as four times of standard deviations (4 σ) when measuring blank samples with 1 min average, and the accuracy was estimated to be ~25%.



### 2.3 Model description

We use GEOS-Chem (version 12.9.3) to quantify the effects of ClNO<sub>2</sub> formation due to heterogeneous reaction of N<sub>2</sub>O<sub>5</sub> with saline dust in China. The model, which includes a detailed representation of coupled ozone-NO<sub>x</sub>-VOCs-aerosol-halogen chemistry (Wang et al., 2021), is driven by MERRA2 (the Modern-Era Retrospective Analysis for Research and Applications, Version 2) assimilated meteorological fields from the NASA Global Modeling and Assimilation Office (GMAO) with native horizontal resolution of 0.25°×0.3125° and 72 vertical levels from the surface to the mesosphere. Our simulation was conducted over East Asia (60°-150°E, 10°S-55°N) at the native resolution with dynamical boundary conditions from a 4°×5° global simulation. Anthropogenic emissions in China are based on the Multiresolution Emission Inventory for China (MEIC) (Zheng et al., 2018) and an inventory of HCl and fine particulate Cl<sup>-</sup> in China (Fu et al., 2018). Natural dust emissions are calculated based on Ridley et al. (2013). A more detailed description of the model and emissions can be found elsewhere (Wang et al., 2020b).

For  $\text{N}_2\text{O}_5$  uptake onto aqueous aerosols, the parameterization in our previous study (Wang et al., 2020b) for  $\gamma(\text{N}_2\text{O}_5)$  and  $\phi(\text{ClNO}_2)$ , which are based on a detail evaluation of different model parameterizations by previous work (McDuffie et al., 2018a; McDuffie et al., 2018b), is used in this study, and more details can be found in the supplement. For  $\text{N}_2\text{O}_5$  uptake on dust aerosol,  $\gamma(\text{N}_2\text{O}_5)$  is always assumed to be 0.02, as recommended previously (Crowley et al., 2010; Tang et al., 2017), and  $\phi(\text{ClNO}_2)$  is assumed to be 0 in the standard case, i.e., no  $\text{ClNO}_2$  is produced in heterogeneous reaction of  $\text{N}_2\text{O}_5$  with mineral dust.

### 3 Results and discussion

Figure 2a shows changes in  $\text{N}_2\text{O}_5$  and  $\text{ClNO}_2$  concentrations during an experiment in which heterogeneous reaction of  $\text{N}_2\text{O}_5$  with sample H1 at 37% RH was studied. As shown in Figure 2a, when the mixed flow was passed through the blank filter (0-10 min),  $\text{N}_2\text{O}_5$  concentrations were measured to be  $\sim 350$  pptv and  $\text{ClNO}_2$  was below the detection limit. The mixed flow was then passed through the particle-loaded filter at  $\sim 10$  min in order to initiate heterogeneous reaction of  $\text{N}_2\text{O}_5$  with sample H1, and significant decrease in  $\text{N}_2\text{O}_5$  concentrations (from  $\sim 350$  to  $\sim 150$  pptv) and increase in  $\text{ClNO}_2$  concentrations (from almost 0 to  $\sim 150$  pptv) were observed, suggesting that heterogeneous interaction with sample H1 substantially consumed  $\text{N}_2\text{O}_5$  and generated  $\text{ClNO}_2$ . In order to check if initial  $\text{N}_2\text{O}_5$  and  $\text{ClNO}_2$  concentrations were stable, during our experiments the mixed flow was switched back to pass through the blank filter from time to time (e.g., at around 40, 75 and 105 min for the experiment displayed in Figure 2a). Indeed, initial  $\text{N}_2\text{O}_5$  and  $\text{ClNO}_2$  concentrations were constant in our experiments, with another two examples shown in Figures 2b and 2c.

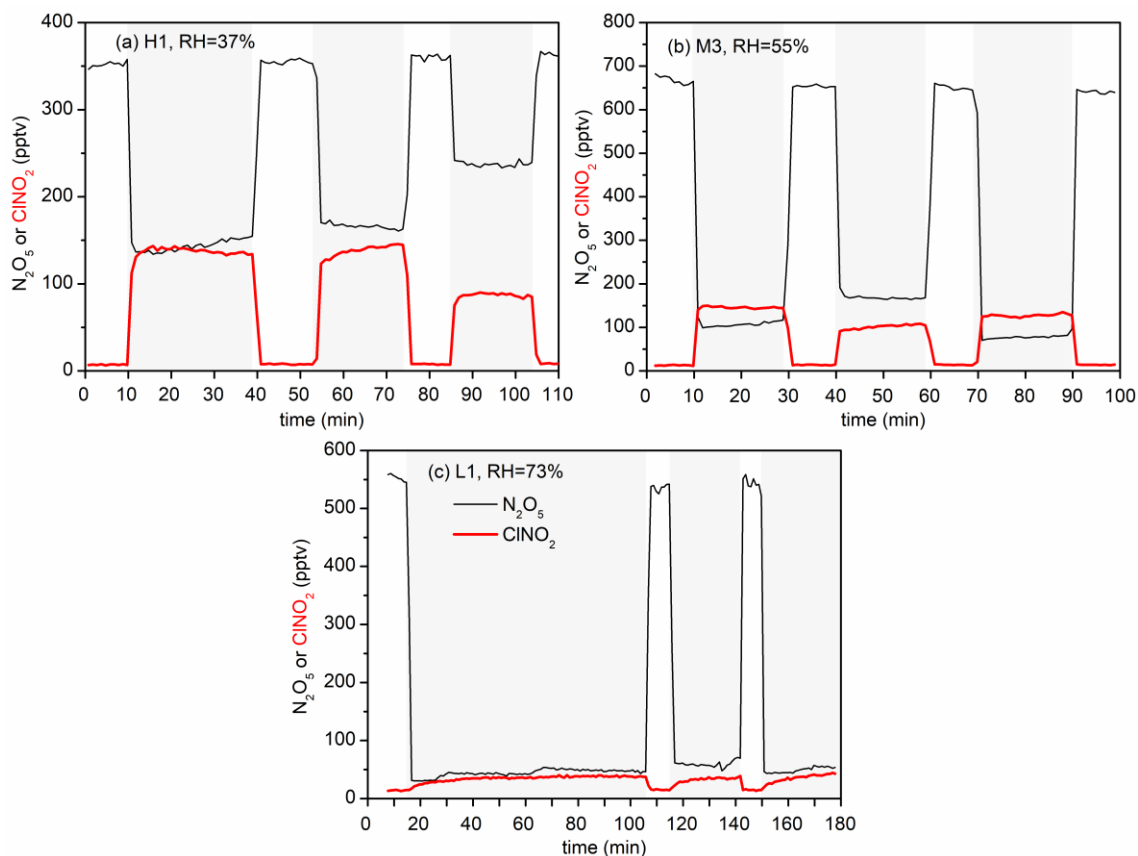


**Figure 2.** Time series for measured  $\text{N}_2\text{O}_5$  and  $\text{ClNO}_2$  concentrations after the mixed flow was passed through the blank filter or the particle-loaded filter: a) H1, 37% RH; b) M3, 55% RH; c) L1, 73% RH. Periods in which the mixed flow was passed through the particle-loaded filter was shadowed with gray.

Figures 2b and 2c show time series of measured  $\text{N}_2\text{O}_5$  and  $\text{ClNO}_2$  concentrations in another two experiments, suggesting that heterogeneous reaction with sample M3 and L1 also led to substantial removal of  $\text{N}_2\text{O}_5$ . However, much less  $\text{ClNO}_2$  was produced for sample M3 and L1, when compared to sample H1 (Figure 2a). The decrease in  $\text{N}_2\text{O}_5$  concentrations,  $\Delta[\text{N}_2\text{O}_5]$ , and the increase in  $\text{ClNO}_2$  concentrations,  $\Delta[\text{ClNO}_2]$ , can be used to calculate  $\text{ClNO}_2$  yields,  $\phi(\text{ClNO}_2)$ , according to Eq. (1).

$$\varphi(\text{ClNO}_2) = \frac{\Delta[\text{ClNO}_2]}{\Delta[\text{N}_2\text{O}_5]} \quad (1)$$

In this work we measured  $\varphi(\text{ClNO}_2)$  for heterogeneous reaction of  $\text{N}_2\text{O}_5$  with eight different saline mineral dust samples at four RH, and each experiment was repeated at least three times. It should be mentioned that during each experiment the measured  $\varphi(\text{ClNO}_2)$  did not vary significantly with time, and therefore an average value of  $\varphi(\text{ClNO}_2)$  was reported for each experiment. Table 2 summarizes measured  $\varphi(\text{ClNO}_2)$  for the eight samples at different RH, and the results are further discussed in the following sections.

**Table 2.** Measured  $\text{ClNO}_2$  yields for heterogeneous uptake of  $\text{N}_2\text{O}_5$  onto saline mineral dust samples at different RH. All the errors given in this work are standard deviations. The uncertainty of RH was  $\pm 2\%$ .

| sample | 18% RH            | 36% RH            | 56% RH            | 75% RH            |
|--------|-------------------|-------------------|-------------------|-------------------|
| H1     | 0.402 $\pm$ 0.138 | 0.663 $\pm$ 0.039 | 0.774 $\pm$ 0.028 | 0.697 $\pm$ 0.311 |
| H2     | 0.560 $\pm$ 0.046 | 0.474 $\pm$ 0.026 | 0.494 $\pm$ 0.042 | 0.378 $\pm$ 0.069 |
| M1     | 0.271 $\pm$ 0.038 | 0.271 $\pm$ 0.030 | 0.418 $\pm$ 0.053 | 0.543 $\pm$ 0.086 |
| M2     | 0.166 $\pm$ 0.018 | 0.246 $\pm$ 0.041 | 0.316 $\pm$ 0.046 | 0.418 $\pm$ 0.052 |
| M3     | 0.223 $\pm$ 0.061 | 0.251 $\pm$ 0.050 | 0.211 $\pm$ 0.025 | 0.120 $\pm$ 0.050 |
| M4     | 0.179 $\pm$ 0.075 | 0.133 $\pm$ 0.007 | 0.205 $\pm$ 0.021 | 0.181 $\pm$ 0.044 |
| L1     | 0.037 $\pm$ 0.006 | 0.030 $\pm$ 0.015 | 0.045 $\pm$ 0.025 | 0.048 $\pm$ 0.008 |
| L2     | 0.012 $\pm$ 0.003 | 0.005 $\pm$ 0.004 | 0.024 $\pm$ 0.042 | 0.041 $\pm$ 0.039 |

### 3.1 $\text{ClNO}_2$ production yields

Figure 3 shows  $\text{ClNO}_2$  yields as a function of RH for the two samples with high chloride content (H1 and H2), and  $\varphi(\text{ClNO}_2)$  were found to be quite high for the two samples. To be more specific, the mass fraction of chloride was 0.3870 for sample H1, and  $\varphi(\text{ClNO}_2)$  were found to increase from 0.402 $\pm$ 0.138 at 18% RH to 0.774 $\pm$ 0.028 at 56% RH, and then slightly decreased to

0.697±0.311 when RH was further increased to 75%. For sample H2, the mass fraction of chloride (0.2145) was lower than sample H1, and  $\phi(\text{ClNO}_2)$  showed a small decrease (or remained relatively constant) when RH was increased from 18% to 56%, ranging from 0.474±0.026 to 0.560±0.046; further increase in RH to 75% resulted in small decrease in  $\phi(\text{ClNO}_2)$  to 0.378±0.069.

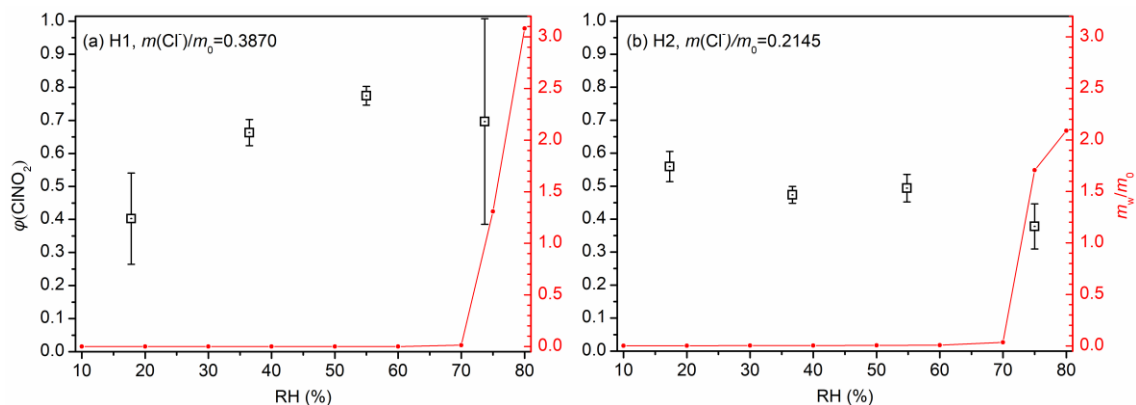


**Figure 3.** Measured  $\text{ClNO}_2$  yields (black symbol) and  $m_w/m_0$  (red line) as a function of RH for (a) H1 and (b) H2. The error bar represents standard deviation, and  $m_w/m_0$  represents normalized mass of particulate water (normalized to the mass of dry particles), which was measured as the relative increase in particle mass at a given RH compared to <1% RH.

$\text{ClNO}_2$  yields are shown in Figure 4 as a function of RH for the two low chloride samples (L1 and L2), and their mass fractions of chloride were <0.01. As shown in Figure 4,  $\phi(\text{ClNO}_2)$  were found to be always <0.05 for the two samples, suggesting that heterogeneous production of  $\text{ClNO}_2$  was very limited, despite substantial removal of  $\text{N}_2\text{O}_5$  due to heterogeneous reaction (with an example shown in Figure 2c). The low  $\phi(\text{ClNO}_2)$  values for sample L1 and L2 could be attributed to their low chloride contents. In addition,  $\phi(\text{ClNO}_2)$  appeared to increase with RH for L1 and L2; however, since the uncertainties associated with  $\phi(\text{ClNO}_2)$  were rather large for these two samples, the dependence of  $\phi(\text{ClNO}_2)$  on RH should be treated in caution.

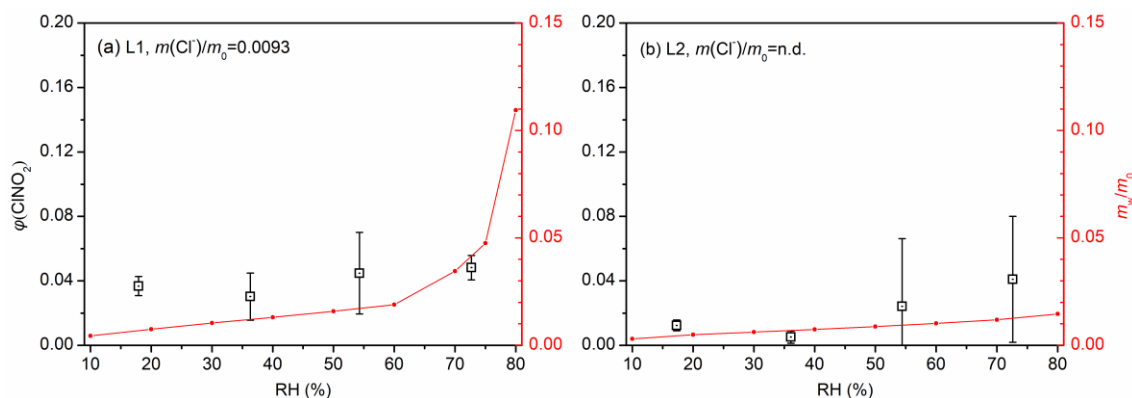


**Figure 4.** Measured  $\text{ClNO}_2$  yields (black symbol) and  $m_w/m_0$  (red line) as a function of RH for (a) L1 and (b) L2. The error bar represents standard deviation, and  $m_w/m_0$  represents normalized mass of particulate water (normalized to the mass of dry particles), which was measured as the relative increase in particle mass at a given RH compared to <1% RH.

We also investigated  $\text{ClNO}_2$  production from heterogeneous reaction of  $\text{N}_2\text{O}_5$  with four samples with medium chloride contents (M1, M2, M3 and M4), and the results are displayed in Figure 5. Mass fractions of chloride were determined to be 0.0508 for M1, 0.034 for M2, 0.0229 for M3 and 0.0095 for M4, respectively.  $\text{ClNO}_2$  yields were found to increase significantly with RH for M1 and M2; more specifically,  $\phi(\text{ClNO}_2)$  increased from  $0.271 \pm 0.038$  at 18% RH to  $0.543 \pm 0.086$  at 75% RH for sample M1, and increased from  $0.166 \pm 0.018$  at 18% RH to  $0.418 \pm 0.0052$  at 75% RH for sample M2. As shown in Figure 5, the dependence of  $\phi(\text{ClNO}_2)$  on RH for the other two medium chloride samples (M3 and M4) were rather different from M1 and M2. For sample M3,  $\phi(\text{ClNO}_2)$  first increased from  $0.223 \pm 0.061$  at 18% RH to  $0.251 \pm 0.050$  at 36% RH, and further increase in RH to 75% caused substantial reduction in  $\phi(\text{ClNO}_2)$ . At last, no significant variation of  $\phi(\text{ClNO}_2)$  with RH (18-75%) was observed for sample M4.

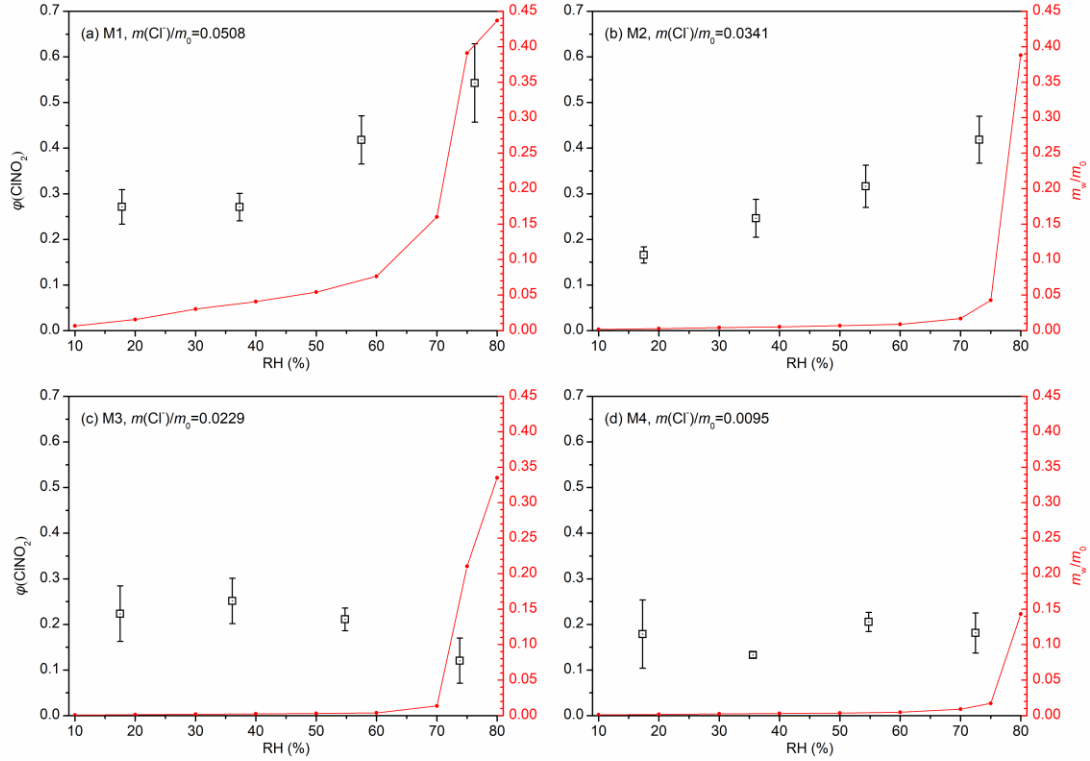


**Figure 5.** Measured  $\text{ClNO}_2$  yields (black symbol) and  $m_w/m_0$  (red line) as a function of RH for (a) M1, (b) M2, (c) M3, and (d) M4. The error bar represents standard deviation, and  $m_w/m_0$  represents normalized mass of particulate water (normalized to the mass of dry particles), which was measured as the relative increase in particle mass at a given RH compared to <1% RH.

### 3.2 The effects of RH

The dependence of  $\phi(\text{ClNO}_2)$  on RH for the eight saline mineral samples we examined, as discussed in Section 3.1, exhibited two interesting features. First, when RH was as low as 18%, large  $\phi(\text{ClNO}_2)$  values ( $>0.2$ ) were observed for four samples (H1, H2, M1 and M3). As the deliquescence RH of NaCl is  $\sim 75\%$ , one may wonder where aqueous chloride, which is necessary for heterogeneous formation of  $\text{ClNO}_2$ , came from at 18% RH. As initially suggested by a previous study (Mitroo et al., 2019), the occurrence of aqueous chloride in saline mineral dust particles at low RH could be due to the presence of  $\text{CaCl}_2$  and  $\text{MgCl}_2$ , which were amorphous under dry



conditions and could take up water at very low RH (Guo et al., 2019). Our previous study (Tang et al., 2019) measured water soluble ions contained by the eight saline mineral dust samples, and as shown in Figure S1, the amounts of water soluble  $\text{Ca}^{2+}$  in the four samples (H1, H2, M1 and M3) with larger  $\phi(\text{ClNO}_2)$  at 18% RH were significantly larger than those in the other four samples (M2, M4, L1 and L2). This observation further supported our deduction that the presence of  $\text{CaCl}_2$  enabled efficient formation of  $\text{ClNO}_2$  at low RH.

The second interesting feature is that as shown in Figures 3-5,  $\phi(\text{ClNO}_2)$  could increase, decrease or remain relatively constant with increase in RH from 18% to 75%. This feature can be understood given the complex mechanisms driving heterogeneous uptake of  $\text{N}_2\text{O}_5$  onto saline mineral dust (Mitroo et al., 2019; Royer et al., 2021): at a given RH,  $\text{N}_2\text{O}_5$  can react with aqueous water, aqueous chloride and insoluble minerals, and only its reaction with aqueous chloride would produce  $\text{ClNO}_2$ . The possible effects of RH on  $\phi(\text{ClNO}_2)$  are discussed below: 1) as RH increases, heterogeneous reactivity of  $\text{N}_2\text{O}_5$  towards insoluble minerals can be enhanced, suppressed or remain largely unchanged (Tang et al., 2012; Tang et al., 2017); 2) increase in RH would lead to further hygroscopic growth and dilution of aqueous solutions, leading to decrease in  $\phi(\text{ClNO}_2)$  in this aspect; 3) the increase in particulate water with RH would cause more chloride to be dissolved into aqueous solutions, and in this aspect increase in RH would promote  $\text{ClNO}_2$  formation. As a result, it is not surprised to observe different dependence of  $\phi(\text{ClNO}_2)$  on RH for different saline mineral dust samples.

### 3.3 Discussion

Figure 6 shows the dependence of  $\phi(\text{ClNO}_2)$  on mass fractions of chloride for the eight samples we examined at four different RH. These samples showed significant variation in

$\phi(\text{ClNO}_2)$ , ranging from  $<0.1$  to  $>0.7$ , and  $\phi(\text{ClNO}_2)$  were largest for the two high chloride samples (H1 and H2), followed by median (M1, M2, M3 and M4) and low chloride samples (L1 and L2). Overall, a positive dependence of  $\phi(\text{ClNO}_2)$  on mass fractions of chloride was observed at each RH. Figure 6 also reveals that the measured  $\phi(\text{ClNO}_2)$  were very sensitive to mass fractions of chloride when the mass fractions of chloride were below 10%. However, as shown in Figure 6, higher chloride contents did not always mean larger  $\phi(\text{ClNO}_2)$ , and similar observations were also reported by previous work (Mitroo et al., 2019; Royer et al., 2021). Furthermore, Figure 6 suggests that when mass fractions of chloride was  $<10\%$ , the dependence of  $\phi(\text{ClNO}_2)$  on Cl contents was stronger at higher RH. This is because increase in RH would promote dissolution of chloride to aqueous water and thus enhance  $\text{ClNO}_2$  formation.

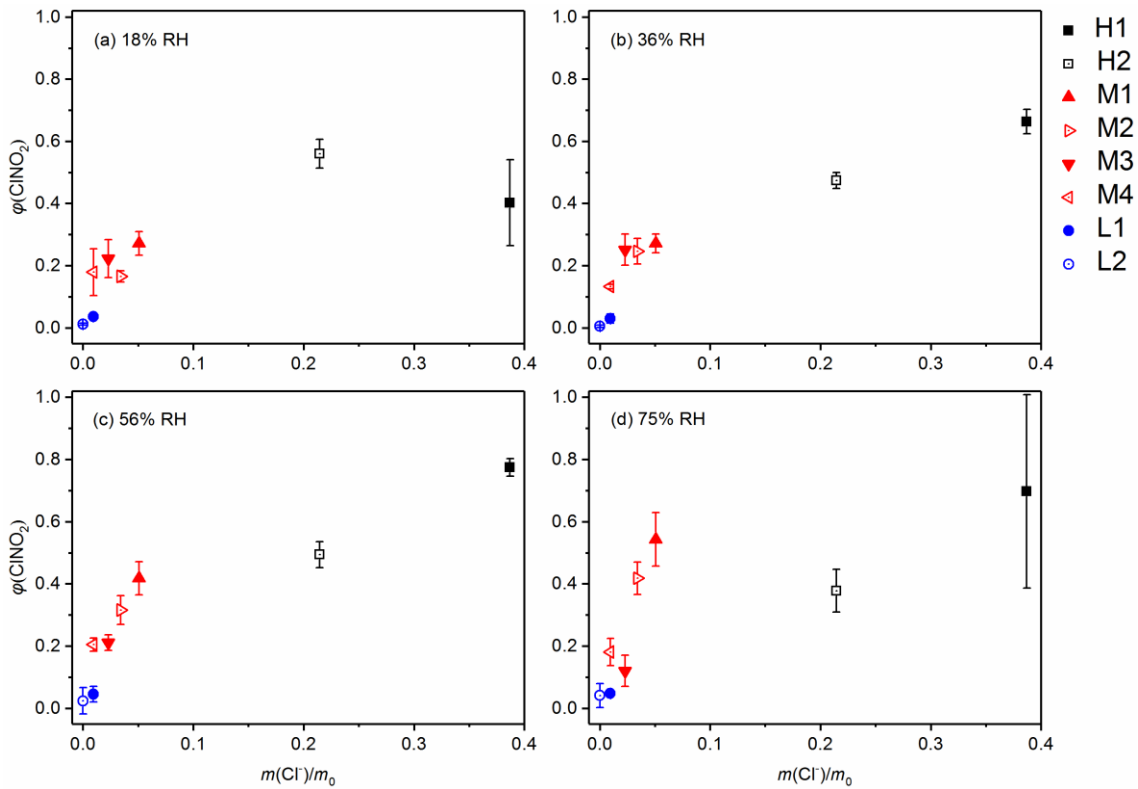


**Figure 6.** Dependence of  $\text{ClNO}_2$  yields on mass fractions of chloride for the eight saline mineral dust samples at a given RH: a) 18% RH; b) 36% RH; c) 56% RH; d) 75% RH.

Two parameterizations have been widely used to predict the dependence of  $\phi(\text{ClNO}_2)$  on chemical compositions and water contents of aqueous aerosol particles (Bertram and Thornton, 2009; Yu et al., 2020). Based on laboratory results, Bertram and Thornton (2009) suggested that  $\text{ClNO}_2$  yields can be calculated using Eq. (2):

$$\phi(\text{ClNO}_2) = \left(1 + \frac{k(\text{H}_2\text{O}) \cdot [\text{H}_2\text{O}_{(\text{aq})}]}{k(\text{Cl}^-) \cdot [\text{Cl}^-]}\right)^{-1} \quad (2)$$

where  $[\text{H}_2\text{O}_{(\text{aq})}]/[\text{Cl}^-]$  is the ratio of molar concentration of  $\text{H}_2\text{O}$  to that of  $\text{Cl}^-$  in aqueous particles, and the value of  $k(\text{H}_2\text{O})/k(\text{Cl}^-)$  was suggested to be  $1/(483 \pm 175)$  (Bertram and Thornton, 2009). Very recently, Yu et al. (2020) examined uptake coefficients of  $\text{N}_2\text{O}_5$  onto ambient aerosol particles at four different sites in China, and suggested that using a value of  $1/(105 \pm 37)$  for  $k(\text{H}_2\text{O})/k(\text{Cl}^-)$  would lead to better agreement between measured and predicted uptake coefficients of  $\text{N}_2\text{O}_5$  (Yu et al., 2020).

The two parameterizations were used in our work to calculate  $\phi(\text{ClNO}_2)$  at 75% RH for the eight saline mineral dust samples we examined.  $[\text{H}_2\text{O}_{(\text{aq})}]/[\text{Cl}^-]$  was calculated from the measured mass growth factors at 75% RH and the mass fractions of chloride, assuming that all the chloride contained by saline mineral dust samples was dissolved into aqueous solutions at 75% RH. The comparison between measured and calculated  $\phi(\text{ClNO}_2)$  is displayed in Figure 7, suggesting that both parameterizations significantly overestimated the measured  $\phi(\text{ClNO}_2)$  for all the eight saline mineral dust samples we investigated. A previous study (Mitroo et al., 2019) investigated  $\phi(\text{ClNO}_2)$  for heterogeneous uptake of  $\text{N}_2\text{O}_5$  onto saline mineral dust samples collected in southwestern USA, and similarly they found that the measured  $\phi(\text{ClNO}_2)$  were significantly smaller than those predicted using the parameterization proposed by Bertram and Thornton (2009).

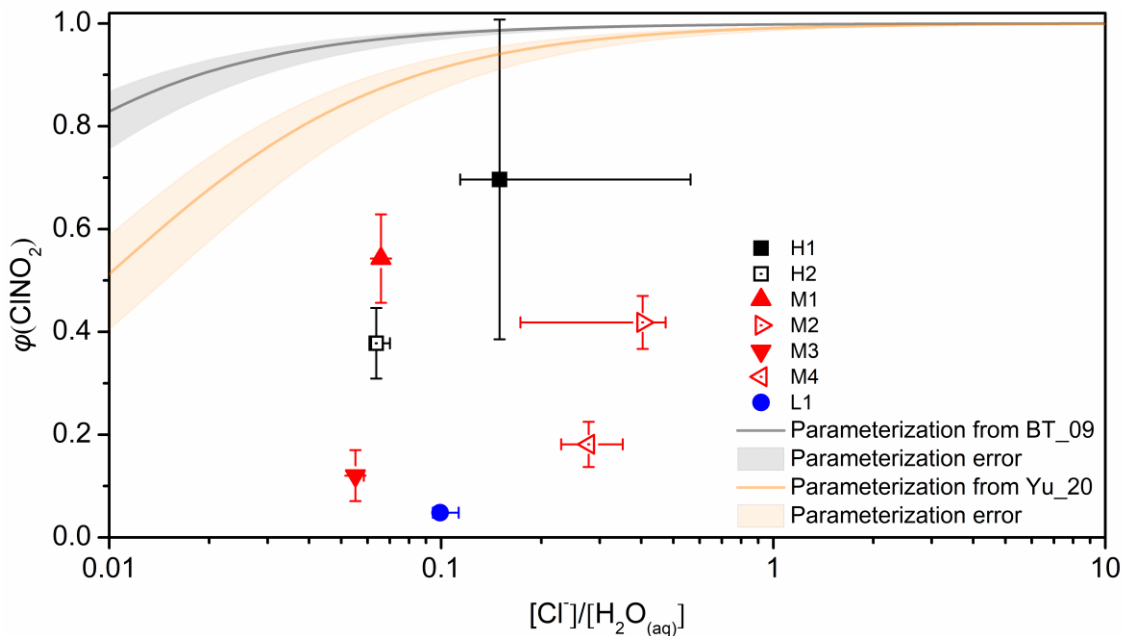


**Figure 7.** Measured and calculated of  $\phi(\text{ClNO}_2)$  at  $75 \pm 2\%$  RH as a function of  $[\text{Cl}^-]/[\text{H}_2\text{O}_{(\text{aq})}]$ . Black and orange curves represent  $\phi(\text{ClNO}_2)$  calculated using the BT\_09 parameterization (Bertram and Thornton, 2009) and the Yu\_20 parameterization (Yu et al., 2020), and the associated errors are represented by the corresponding shadows.

The observed discrepancies between measured and predicted  $\phi(\text{ClNO}_2)$  can be caused by several reasons. First, even at  $\sim 75\%$  RH (the highest RH at which our experiments were conducted), chloride contained in saline mineral dust may not be fully dissolved, and therefore our calculation may overestimate  $[\text{Cl}^-]/[\text{H}_2\text{O}_{(\text{aq})}]$  and thus also overestimate  $\phi(\text{ClNO}_2)$ . This effect should not be large as significant water uptake was observed at  $\sim 75\%$  RH for saline mineral dust sample we examined (Figures 3-5). Second, perhaps more importantly, saline mineral dust samples contain substantial amounts of insoluble minerals, and some of these minerals, such as clays, are very reactive towards  $\text{N}_2\text{O}_5$  (Tang et al., 2017), and only nitrate but no  $\text{ClNO}_2$  was formed (Seisel et al., 2005; Karagulian et al., 2006; Tang et al., 2012). However, the two parameterizations did not take into account heterogeneous reaction of  $\text{N}_2\text{O}_5$  with insoluble minerals, and as a result would

inevitably overestimate  $\varphi(\text{ClNO}_2)$ . At last, our calculations assumed internal mixing, but inter- and intra-particle heterogeneity of saline mineral dust particles could also contribute to the observed gap between measured and calculated  $\varphi(\text{ClNO}_2)$ . For example, a wintertime field campaign at Ann Arbor (Michigan, USA) (McNamara et al., 2020) showed that **due to** nonhomogeneous chloride distribution across road salt aerosol particles, **observed  $\varphi(\text{ClNO}_2)$  were significantly smaller than predicted values**. The comparison between measured and predicted  $\varphi(\text{ClNO}_2)$  suggested that while heterogeneous uptake of  $\text{N}_2\text{O}_5$  onto saline mineral dust could be an important source of inland  $\text{ClNO}_2$ , underlying mechanisms which affect heterogeneous production of  $\text{ClNO}_2$  from saline mineral dust have not been well elucidated.

#### **4 Atmospheric implications**

We consider  $\text{ClNO}_2$  formation in heterogeneous uptake of  $\text{N}_2\text{O}_5$  onto dust aerosol in GEOS-Chem to explore its implications. Since  $\text{Cl}^-$  concentration in mineral dust is not well known and currently we are not able to parameterize  $\varphi(\text{ClNO}_2)$  for mineral dust (as discussed in Section 3.3), we use a fixed  $\varphi(\text{ClNO}_2)$  value of 0.1 in our simulation. This value, **which is at the low end of our measured range of  $\varphi(\text{ClNO}_2)$  ( $<0.05$  to  $\sim 0.77$ )**, is higher than those determined in our work for low chloride samples but lower than those for medium chloride samples. **The purpose of our modeling work, is to preliminarily assess whether  $\text{N}_2\text{O}_5$  uptake onto saline dust as a potential source of  $\text{ClNO}_2$  may have important effects on tropospheric chemistry**. We focus on simulations on 2-7 May 2017, during which a large dust event took place in East Asia. It caused high concentrations of dust aerosols with maximum hourly concentration higher than  $1000 \mu\text{g}/\text{m}^3$  over a wide area in China (Zhang et al., 2018), which are also well captured by our simulations (Figure S2).

Figure 8 shows the weekly mean values of the nighttime maximum surface  $\text{ClNO}_2$  mixing ratios and the contribution of heterogeneous reaction of  $\text{N}_2\text{O}_5$  with dust aerosol to  $\text{ClNO}_2$  over 2-7 May 2017. The impact of  $\text{N}_2\text{O}_5$  uptake onto dust aerosol is calculated as the difference between the standard case in which  $\phi(\text{ClNO}_2)$  is assumed to be 0 for  $\text{N}_2\text{O}_5$  uptake onto dust aerosol and the case in which  $\phi(\text{ClNO}_2)$  is assumed to be 0.1. Due to large diurnal variations and near-zero mixing ratios of  $\text{ClNO}_2$  in the daytime, we use the mean nighttime maximum value for  $\text{ClNO}_2$ , following previous standard practice (Wang et al., 2019). The largest impact on  $\text{ClNO}_2$  is found in Central China, where weekly mean nighttime maximum surface  $\text{ClNO}_2$  mixing ratios are increased by 85 pptv, due to heavy impact of dust aerosol transported from the north and high  $\text{NO}_x$  emissions in this region. Even larger effects (up to 240 pptv increase in  $\text{ClNO}_2$ ) can be found on some individual days, as shown in Figures S3 and S4. These results suggest that  $\text{N}_2\text{O}_5$  uptake onto dust could be an important source for tropospheric  $\text{ClNO}_2$  over Central and Northeast China, where  $\text{ClNO}_2$  formation is conventionally believed to be limited due to relatively low aerosol chloride levels from sea salts and anthropogenic sources.

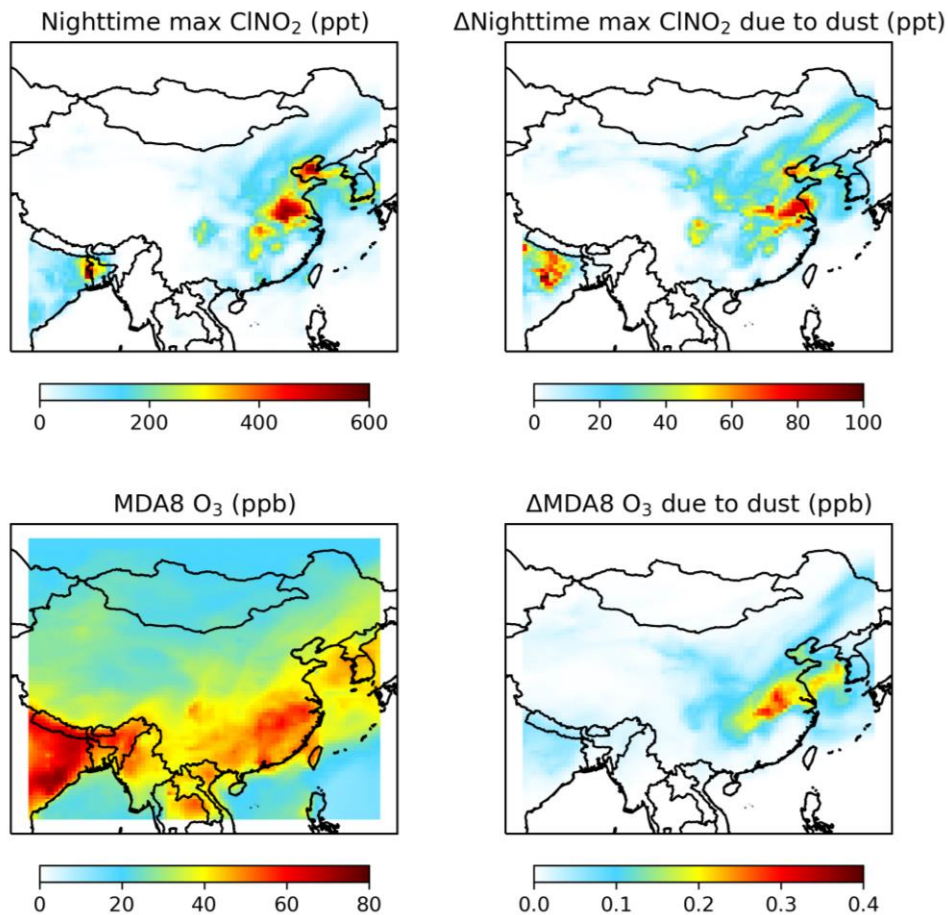


**Figure 8.** Modeled weekly mean mixing ratios of nighttime maximum  $\text{ClNO}_2$  (upper panels) and maximum daily 8-h average (MDA8) ozone (bottom panels) in surface air over China during 2-7 May 2017. The left panels show simulated mixing ratios in our standard case in which  $\phi(\text{ClNO}_2)$  is assumed to be 0 for  $\text{N}_2\text{O}_5$  uptake onto dust aerosol. The right panels show impacts of  $\text{ClNO}_2$  formation due to  $\text{N}_2\text{O}_5$  uptake onto dust, calculated as the difference between the standard case and the case in which  $\phi(\text{ClNO}_2)$  is assumed to be 0.1 for  $\text{N}_2\text{O}_5$  uptake onto dust.

Figure 8 also shows the effect of  $\text{ClNO}_2$  formation due to heterogeneous reaction of  $\text{N}_2\text{O}_5$  with dust aerosol on the daily maximum 8-h average (MDA8) ozone mixing ratios in the surface air over China during the same period. MDA8 ozone mixing ratios are increased by up to 0.32

ppbv after considering mineral dust as an additional source of ClNO<sub>2</sub>. Our simulation assumes a low value of  $\varphi(\text{ClNO}_2)$  in our measured range (<0.05 to ~0.77), and is conducted in summer when ClNO<sub>2</sub> is more difficult to be accumulated due to short night (compared to winter and spring with long nights). We expect that its impacts on ClNO<sub>2</sub> and ozone could be larger for dust events in winter and spring.

## 5 Conclusions

It has been widely recognized that nitryl chloride (ClNO<sub>2</sub>), produced by heterogeneous reaction of N<sub>2</sub>O<sub>5</sub> with chloride-containing aerosols, could significantly affect atmospheric oxidation capacity. However, heterogeneous formation of tropospheric ClNO<sub>2</sub> in inland regions in China has not been well elucidated. In this work, we investigated ClNO<sub>2</sub> formation in heterogeneous reaction of N<sub>2</sub>O<sub>5</sub> with eight saline mineral dust samples collected from different regions in China as a function of RH (18-75%). Significant production of ClNO<sub>2</sub> was observed for some of the saline mineral dust samples examined, and ClNO<sub>2</sub> yields,  $\varphi(\text{ClNO}_2)$ , were determined to span from <0.05 to 0.77, depending on chemical compositions of saline mineral dust samples and RH. In general a positive dependence of  $\varphi(\text{ClNO}_2)$  on mass fractions of particulate chloride was observed at each RH, but higher particulate chloride content did not always mean larger  $\varphi(\text{ClNO}_2)$ . On the other hand, increase in RH could increase, reduce or have no significant impacts on  $\varphi(\text{ClNO}_2)$ , revealing the complex mechanisms which drive heterogeneous uptake of N<sub>2</sub>O<sub>5</sub> onto saline mineral dust.

Two widely-used parameterizations (Bertram and Thornton, 2009; Yu et al., 2020) were used to estimate  $\varphi(\text{ClNO}_2)$  at 75% RH for the eight saline mineral dust samples we investigated. Both parameterizations were found to significantly overestimate the measured  $\varphi(\text{ClNO}_2)$ , and we



suggested that the discrepancies between measured and predicted  $\varphi(\text{ClNO}_2)$  could be due to incomplete dissolution of particulate chloride, heterogeneous reaction of  $\text{N}_2\text{O}_5$  with insoluble minerals, and/or inter- and intra-particle heterogeneity of saline mineral dust particles.

Assuming a  $\varphi(\text{ClNO}_2)$  value of 0.1 for heterogeneous reaction of  $\text{N}_2\text{O}_5$  with mineral dust, we use GEOS-Chem to assess the impact of this reaction on tropospheric  $\text{ClNO}_2$  and  $\text{O}_3$  in China during a severe dust event on 2-7 May 2017. It is found that after taking into  $\text{ClNO}_2$  production due to  $\text{N}_2\text{O}_5$  uptake onto mineral dust aerosol, weekly mean nighttime maximum  $\text{ClNO}_2$  mixing ratios could be increased by up to 85 pptv during this period and the daily maximum 8-h average  $\text{O}_3$  mixing ratios were increased by up to 0.32 ppbv.

In summary, our work shows that heterogeneous reaction of  $\text{N}_2\text{O}_5$  with saline mineral dust can be an important source for tropospheric  $\text{ClNO}_2$  in inland China. This reaction may also important for tropospheric  $\text{ClNO}_2$  production in many other regions over the world, as the occurrence of saline mineral dust aerosols has been reported in various locations, such as Iran (Gholampour et al., 2015), United States (Blank et al., 1999; Pratt et al., 2010; Jordan et al., 2015; Frie et al., 2017), and Argentina (Bucher and Stein, 2016). Currently our limited knowledge precludes quantitative prediction of heterogeneous  $\text{ClNO}_2$  production from saline mineral dust, and further investigation is thus warranted.

## **Appendix. $\text{N}_2\text{O}_5$ and $\text{ClNO}_2$ calibration**

To calibrate CIMS measurements of  $\text{N}_2\text{O}_5$ , a mixed flow containing  $\text{N}_2\text{O}_5$ , which was produced via  $\text{O}_3$  oxidation of  $\text{NO}_2$ , was sampled into the CIMS instrument, and  $\text{N}_2\text{O}_5$  was quantified using the normalized intensities of  $\text{I}(\text{N}_2\text{O}_5)^-$  clusters,  $f(\text{N}_2\text{O}_5)$ , defined as the ratio of signal intensity (cps) of  $\text{I}(\text{N}_2\text{O}_5)^-$  to that of the total reagent ions, i.e.  $\text{I}^-$  and  $\text{I}(\text{H}_2\text{O})^-$ .  $\text{N}_2\text{O}_5$

concentrations in the mixed flow were quantified using cavity-enhanced absorption spectroscopy (CEAS) (Wang et al., 2017a), with a detection limit of 2.7 pptv in 5 s and an uncertainty of ~25%. RH of the mixed flow was varied during the calibration in order to determine the CIMS sensitivity for  $\text{N}_2\text{O}_5$  at different RH, and the results are displayed in Figure A1. The sensitivity for  $\text{N}_2\text{O}_5$  first increased with RH, reaching the maximum value at ~40% RH, and then decreased with further increase in RH.

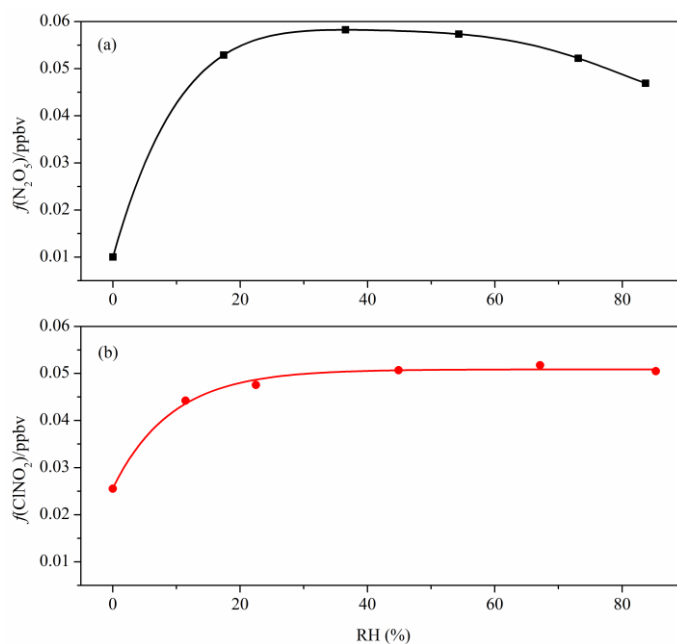


**Figure A1.** CIMS sensitivities as a function of RH for (a)  $\text{N}_2\text{O}_5$  and (b)  $\text{ClNO}_2$ .

To calibrate CIMS measurements of  $\text{ClNO}_2$ , a nitrogen flow (6 mL/min) containing 10 ppmv  $\text{Cl}_2$  was passed over a slurry containing  $\text{NaNO}_2$  and  $\text{NaCl}$  to produce  $\text{ClNO}_2$  (Thaler et al., 2011), and  $\text{NaCl}$  was included in the slurry in order to minimize the formation of  $\text{NO}_2$  as a byproduct. The mixed flow containing  $\text{ClNO}_2$  was then conditioned to a given RH and sampled into the CIMS instrument; similar to  $\text{N}_2\text{O}_5$ ,  $\text{ClNO}_2$  was quantified using the normalized intensities of  $\text{I}(\text{ClNO}_2)^-$  clusters,  $f(\text{ClNO}_2)$ , defined as the ratio of signal intensity (cps) of  $\text{I}(\text{ClNO}_2)^-$  to that of the total

reagent ions. To quantify ClNO<sub>2</sub>, the mixed flow was delivered directly into a cavity attenuated phase shift spectroscopy instrument (CAPS, Model N500, Teledyne API) to measure background NO<sub>2</sub> concentrations; after that, the mixed flow was delivered through a thermal dissociation model at 365 °C to fully decompose ClNO<sub>2</sub> to NO<sub>2</sub>, and the total NO<sub>2</sub> concentrations were then determined using CAPS. The differences in the measured NO<sub>2</sub> concentrations with and without thermal dissociation was equal to ClNO<sub>2</sub> concentrations. The CAPS instrument had a detection limit of 0.2 ppbv in 1 min for NO<sub>2</sub> and an uncertainty of ~10%. As shown in Figure A1, the sensitivity for ClNO<sub>2</sub> increased with RH up to 40%, and showed little variation with further increase in RH.

#### **Data availability**

Data used in this paper can be found in the main text or supplement. GEOS-Chem model is available at GEOS-Chem repository (<http://www.geos-chem.org>).

#### **Competing interests**

The authors declare that they have no conflict of interest.

#### **Author contribution**

**Haichao Wang:** investigation, formal analysis, writing-original draft, writing – review & editing;

**Chao Peng:** investigation, formal analysis, writing-original draft, writing – review & editing;

**Xuan Wang:** investigation, formal analysis, writing-original draft, writing – review & editing;

**Shengrong Lou:** resources; **Keding Lu:** resources, supervision; **Guicheng Gan:** investigation;

**Xiaohong Jia:** investigation; **Xiaorui Chen:** investigation; **Jun Chen:** supervision; **Hongli Wang:**

resources; **Shaojia Fan:** resources; **Xinming Wang:** resources; **Mingjin Tang:** conceptualization,

formal analysis, resources, supervision, writing-original draft, writing-review & editing.

## Financial support

This work was funded by National Natural Science Foundation of China (41907185, 91744204 and 42022050), Ministry of Science and Technology of China (2018YFC0213901), Guangdong Basic and Applied Basic Research Fund Committee (2020B1515130003), National State Environmental Protection Key Laboratory of Formation and Prevention of Urban Air Pollution Complex (CX2020080094 and CX2020080578), Guangdong Foundation for Program of Science and Technology Research (2019B121205006 and 2020B1212060053), Guangdong Science and Technology Department (2017GC010501) and CAS Pioneer Hundred Talents program.

## Reference

- Abuduwailli, J., Gabchenko, M. V., and Xu, J.: Eolian transport of salts - A case study in the area of Lake Ebinur (Xinjiang, Northwest China), *Journal of Arid Environments*, 72, 1843-1852, 2008.
- Ahern, A., Goldberger, L., Jahl, L., Thornton, J., and Sullivan, R. C.: Production of N<sub>2</sub>O<sub>5</sub> and ClNO<sub>2</sub> through nocturnal processing of biomass-burning aerosol, *Environmental science & technology*, 52, 550-559, 2017.
- Atkinson, R., and Arey, J.: Atmospheric degradation of volatile organic compounds, *Chemical Reviews*, 103, 4605-4638, 2003.
- Atkinson, R., Baulch, D. L., Cox, R. A., Crowley, J. N., Hampson, R. F., Hynes, R. G., Jenkin, M. E., Rossi, M. J., and Troe, J.: Evaluated kinetic and photochemical data for atmospheric chemistry: Volume II - gas phase reactions of organic species, *Atmospheric Chemistry and Physics*, 6, 3625-4055, 2006.
- Bannan, T. J., Booth, A. M., Bacak, A., Muller, J. B. A., Leather, K. E., Le Breton, M., Jones, B., Young, D., Coe, H., Allan, J., Visser, S., Slowik, J. G., Furger, M., Prevot, A. S. H., Lee, J., Dunmore, R. E., Hopkins, J. R., Hamilton, J. F., Lewis, A. C., Whalley, L. K., Sharp, T., Stone, D., Heard, D. E., Fleming, Z. L., Leigh, R., Shallcross, D. E., and Percival, C. J.: The first UK measurements of nitryl chloride using a chemical ionization mass spectrometer in central London in the summer of 2012, and an investigation of the role of Cl atom oxidation, *Journal of Geophysical Research-Atmospheres*, 120, 5638-5657, 2015.
- Bannan, T. J., Khan, M. A. H., Le Breton, M., Priestley, M., Worrall, S. D., Bacak, A., Marsden, N. A., Lowe, D., Pitt, J., Shallcross, D. E., and Percival, C. J.: A Large Source of Atomic Chlorine From ClNO<sub>2</sub> Photolysis at a UK Landfill Site, *Geophysical Research Letters*, 46, 8508-8516, 2019.
- Bertram, T. H., and Thornton, J. A.: Toward a general parameterization of N<sub>2</sub>O<sub>5</sub> reactivity on aqueous particles: the competing effects of particle liquid water, nitrate and chloride, *Atmospheric Chemistry And Physics*, 9, 8351-8363, 2009.

- Blank, R. R., Young, J. A., and Allen, F. L.: Aeolian dust in a saline playa environment, Nevada, USA, *Journal of Arid Environments*, 41, 365-381, 1999.
- Bucher, E. H., and Stein, A. F.: Large Salt Dust Storms Follow a 30-Year Rainfall Cycle in the Mar Chiquita Lake (Cordoba, Argentina), *Plos One*, 11, 2016.
- Crowley, J. N., Ammann, M., Cox, R. A., Hynes, R. G., Jenkin, M. E., Mellouki, A., Rossi, M. J., Troe, J., and Wallington, T. J.: Evaluated kinetic and photochemical data for atmospheric chemistry: Volume V – heterogeneous reactions on solid substrates, *Atmos. Chem. Phys.*, 10, 9059-9223, 2010.
- Eger, P. G., Friedrich, N., Schuladen, J., Shenolikar, J., Fischer, H., Tadic, I., Harder, H., Martinez, M., Rohloff, R., Tauer, S., Drewnick, F., Fachinger, F., Brooks, J., Darbyshire, E., Sciare, J., Pikridas, M., Lelieveld, J., and Crowley, J. N.: Shipborne measurements of ClNO<sub>2</sub> in the Mediterranean Sea and around the Arabian Peninsula during summer, *Atmospheric Chemistry and Physics*, 19, 12121-12140, 2019.
- Faxon, C. B., Bean, J. K., and Hildebrandt Ruiz, L.: Inland Concentrations of Cl<sub>2</sub> and ClNO<sub>2</sub> in Southeast Texas Suggest Chlorine Chemistry Significantly Contributes to Atmospheric Reactivity, *Atmosphere*, 6, 1487-1506, 2015.
- Fountoukis, C., and Nenes, A.: ISORROPIA II: a computationally efficient thermodynamic equilibrium model for K<sup>+</sup>-Ca<sup>2+</sup>-Mg<sup>2+</sup>-NH<sub>4</sub><sup>(+)</sup>-Na<sup>+</sup>-SO<sub>4</sub><sup>2-</sup>-NO<sub>3</sub><sup>-</sup>-Cl<sup>-</sup>-H<sub>2</sub>O aerosols, *Atmospheric Chemistry and Physics*, 7, 4639-4659, 2007.
- Frie, A. L., Dingle, J. H., Ying, S. C., and Bahreini, R.: The Effect of a Receding Saline Lake (The Salton Sea) on Airborne Particulate Matter Composition, *Environmental Science & Technology*, 51, 8283-8292, 2017.
- Fu, X., Wang, T., Wang, S., Zhang, L., Cai, S., Xing, J., and Hao, J.: Anthropogenic Emissions of Hydrogen Chloride and Fine Particulate Chloride in China, *Environ Sci Technol*, 52, 1644-1654, 2018.
- Gaston, C. J., Pratt, K. A., Suski, K. J., May, N. W., Gill, T. E., and Prather, K. A.: Laboratory Studies of the Cloud Droplet Activation Properties and Corresponding Chemistry of Saline Playa Dust, *Environmental Science & Technology*, 51, 1348-1356, 2017.
- Gaston, C. J.: Re-examining Dust Chemical Aging and Its Impacts on Earth's Climate, *Accounts of Chemical Research*, 53, 1005-1013, 2020.
- Gholampour, A., Nabizadeh, R., Hassanvand, M. S., Taghipour, H., Nazmara, S., and Mahvi, A. H.: Characterization of saline dust emission resulted from Urmia Lake drying, *Journal of Environmental Health Science and Engineering*, 13, 2015.
- Gillette, D., Stensland, G., Williams, A., Barnard, W., Gatz, D., Sinclair, P., and Johnson, T.: Emissions of alkaline elements calcium, magnesium, potassium, and sodium from open sources in the contiguous United States, *Global Biogeochemical Cycles*, 6, 437-457, 1992.
- Gu, W., Li, Y., Zhu, J., Jia, X., Lin, Q., Zhang, G., Ding, X., Song, W., Bi, X., Wang, X., and Tang, M.: Investigation of water adsorption and hygroscopicity of atmospherically relevant particles using a commercial vapor sorption analyzer, *Atmospheric Measurement Techniques*, 10, 3821-3832, 2017.
- Guo, L., Gu, W., Peng, C., Wang, W., Li, Y. J., Zong, T., Tang, Y., Wu, Z., Lin, Q., Ge, M., Zhang, G., Hu, M., Bi, X., Wang, X., and Tang, M.: A comprehensive study of hygroscopic properties of calcium- and magnesium-containing salts: implication for hygroscopicity of mineral dust and sea salt aerosols, *Atmospheric Chemistry and Physics*, 19, 2115-2133, 2019.
- Jia, X., Gu, W., Peng, C., Li, R., Chen, L., Wang, H., Wang, H., Wang, X., and Tang, M.: Heterogeneous reaction of CaCO<sub>3</sub> with NO<sub>2</sub> at different relative humidities: Kinetics,

mechanisms, and impacts on aerosol hygroscopicity, *Journal of Geophysical Research-Atmospheres*, 126, e2021JD034826, 2021.

Jordan, C. E., Pszenny, A. A. P., Keene, W. C., Cooper, O. R., Deegan, B., Maben, J., Routhier, M., Sander, R., and Young, A. H.: Origins of aerosol chlorine during winter over north central Colorado, USA, *Journal of Geophysical Research-Atmospheres*, 120, 678-694, 2015.

Karagulian, F., Santschi, C., and Rossi, M. J.: The heterogeneous chemical kinetics of N<sub>2</sub>O<sub>5</sub> on CaCO<sub>3</sub> and other atmospheric mineral dust surrogates, *Atmospheric Chemistry and Physics*, 6, 1373-1388, 2006.

Kercher, J. P., Riedel, T. P., and Thornton, J. A.: Chlorine activation by N<sub>2</sub>O<sub>5</sub>: simultaneous, in situ detection of ClNO<sub>2</sub> and N<sub>2</sub>O<sub>5</sub> by chemical ionization mass spectrometry, *Atmospheric Measurement Techniques*, 2, 193-204, 2009.

Le Breton, M., Hallquist, A. M., Pathak, R. K., Simpson, D., Wang, Y., Johansson, J., Zheng, J., Yang, Y., Shang, D., Wang, H., Liu, Q., Chan, C., Wang, T., Bannan, T. J., Priestley, M., Percival, C. J., Shallcross, D. E., Lu, K., Guo, S., Hu, M., and Hallquist, M.: Chlorine oxidation of VOCs at a semi-rural site in Beijing: significant chlorine liberation from ClNO<sub>2</sub> and subsequent gas- and particle-phase Cl-VOC production, *Atmospheric Chemistry and Physics*, 18, 13013-13030, 2018.

Li, R., Jia, X., Wang, F., Ren, Y., Wang, X., Zhang, H., Li, G., Wang, X., and Tang, M.: Heterogeneous reaction of NO<sub>2</sub> with hematite, goethite and magnetite: Implications for nitrate formation and iron solubility enhancement, *Chemosphere*, 242, 125273-125273, 2020.

Lu, K., Guo, S., Tan, Z., Wang, H., Shang, D., Liu, Y., Li, X., Wu, Z., Hu, M., and Zhang, Y.: Exploring atmospheric free-radical chemistry in China: the self-cleansing capacity and the formation of secondary air pollution, *National Science Review*, 6, 579-594, 2019.

McDuffie, E. E., Fibiger, D. L., Dube, W. P., Hilfiker, F. L., Lee, B. H., Jaegle, L., Guo, H., Weber, R. J., Reeves, J. M., Weinheimer, A. J., Schroder, J. C., Campuzano-Jost, P., Jimenez, J. L., Dibb, J. E., Veres, P., Ebben, C., Sparks, T. L., Wooldridge, P. J., Cohen, R. C., Campos, T., Hall, S. R., Ullmann, K., Roberts, J. M., Thornton, J. A., and Brown, S. S.: ClNO<sub>2</sub> Yields From Aircraft Measurements During the 2015 WINTER Campaign and Critical Evaluation of the Current Parameterization, *Journal of Geophysical Research-Atmospheres*, 123, 12994-13015, 2018a.

McDuffie, E. E., Fibiger, D. L., Dube, W. P., Lopez-Hilfiker, F., Lee, B. H., Thornton, J. A., Shah, V., Jaegle, L., Guo, H., Weber, R. J., Reeves, J. M., Weinheimer, A. J., Schroder, J. C., Campuzano-Jost, P., Jimenez, J. L., Dibb, J. E., Veres, P., Ebben, C., Sparks, T. L., Wooldridge, P. J., Cohen, R. C., Hornbrook, R. S., Apel, E. C., Campos, T., Hall, S. R., Ullmann, K., and Brown, S. S.: Heterogeneous N<sub>2</sub>O<sub>5</sub> Uptake During Winter: Aircraft Measurements During the 2015 WINTER Campaign and Critical Evaluation of Current Parameterizations, *Journal of Geophysical Research-Atmospheres*, 123, 4345-4372, 2018b.

McNamara, S. M., Kolesar, K. R., Wang, S., Kirpes, R. M., May, N. W., Gunch, M. J., Cook, R. D., Fuentes, J. D., Hornbrook, R. S., Apel, E. C., China, S., Laskin, A., and Pratt, K. A.: Observation of Road Salt Aerosol Driving Inland Wintertime Atmospheric Chlorine Chemistry, *Acs Central Science*, 6, 684-694, 2020.

Mielke, L. H., Furgeson, A., and Osthoff, H. D.: Observation of ClNO<sub>2</sub> in a Mid-Continental Urban Environment, *Environmental Science & Technology*, 45, 8889-8896, 2011.

Mielke, L. H., Furgeson, A., Odame-Ankrah, C. A., and Osthoff, H. D.: Ubiquity of ClNO<sub>2</sub> in the urban boundary layer of Calgary, Alberta, Canada, *Canadian Journal of Chemistry*, 94, 414-423, 2016.

- Mitroo, D., Gill, T. E., Haas, S., Pratt, K. A., and Gaston, C. J.: ClNO<sub>2</sub> Production from N<sub>2</sub>O<sub>5</sub> Uptake on Saline Playa Dusts: New Insights into Potential Inland Sources of ClNO<sub>2</sub>, *Environ Sci Technol*, 53, 7442-7452, 2019.
- Osthoff, H. D., Roberts, J. M., Ravishankara, A. R., Williams, E. J., Lerner, B. M., Sommariva, R., Bates, T. S., Coffman, D., Quinn, P. K., Dibb, J. E., Stark, H., Burkholder, J. B., Talukdar, R. K., Meagher, J., Fehsenfeld, F. C., and Brown, S. S.: High levels of nitryl chloride in the polluted subtropical marine boundary layer, *Nature Geoscience*, 1, 324-328, 2008.
- Osthoff, H. D., Odame-Ankrah, C. A., Taha, Y. M., Tokarek, T. W., Schiller, C. L., Haga, D., Jones, K., and Vingarzan, R.: Low levels of nitryl chloride at ground level: nocturnal nitrogen oxides in the Lower Fraser Valley of British Columbia, *Atmospheric Chemistry and Physics*, 18, 6293-6315, 2018.
- Phillips, G. J., Tang, M. J., Thieser, J., Brickwedde, B., Schuster, G., Bohn, B., Lelieveld, J., and Crowley, J. N.: Significant concentrations of nitryl chloride observed in rural continental Europe associated with the influence of sea salt chloride and anthropogenic emissions, *Geophysical Research Letters*, 39, 2012.
- Pratt, K. A., Twohy, C. H., Murphy, S. M., Moffet, R. C., Heymsfield, A. J., Gaston, C. J., DeMott, P. J., Field, P. R., Henn, T. R., Rogers, D. C., Gilles, M. K., Seinfeld, J. H., and Prather, K. A.: Observation of playa salts as nuclei in orographic wave clouds, *Journal of Geophysical Research-Atmospheres*, 115, 2010.
- Ridley, D. A., Heald, C. L., Pierce, J. R., and Evans, M. J.: Toward resolution-independent dust emissions in global models: Impacts on the seasonal and spatial distribution of dust, *Geophysical Research Letters*, 40, 2873-2877, 2013.
- Riedel, T. P., Bertram, T. H., Crisp, T. A., Williams, E. J., Lerner, B. M., Vlasenko, A., Li, S.-M., Gilman, J., de Gouw, J., Bon, D. M., Wagner, N. L., Brown, S. S., and Thornton, J. A.: Nitryl Chloride and Molecular Chlorine in the Coastal Marine Boundary Layer, *Environmental Science & Technology*, 46, 10463-10470, 2012.
- Riedel, T. P., Wagner, N. L., Dube, W. P., Middlebrook, A. M., Young, C. J., Ozturk, F., Bahreini, R., VandenBoer, T. C., Wolfe, D. E., Williams, E. J., Roberts, J. M., Brown, S. S., and Thornton, J. A.: Chlorine activation within urban or power plant plumes: Vertically resolved ClNO<sub>2</sub> and Cl<sub>2</sub> measurements from a tall tower in a polluted continental setting, *Journal of Geophysical Research-Atmospheres*, 118, 8702-8715, 2013.
- Riedel, T. P., Wolfe, G. M., Danas, K. T., Gilman, J. B., Kuster, W. C., Bon, D. M., Vlasenko, A., Li, S. M., Williams, E. J., Lerner, B. M., Veres, P. R., Roberts, J. M., Holloway, J. S., Lefer, B., Brown, S. S., and Thornton, J. A.: An MCM modeling study of nitryl chloride (ClNO<sub>2</sub>) impacts on oxidation, ozone production and nitrogen oxide partitioning in polluted continental outflow, *Atmospheric Chemistry and Physics*, 14, 3789-3800, 2014.
- Royer, H. M., Mitroo, D., Hayes, S. M., Haas, S. M., Pratt, K. A., Blackwelder, P. L., Gill, T. E., and Gaston, C. J.: The Role of Hydrates, Competing Chemical Constituents, and Surface Composition on ClNO<sub>2</sub> Formation, *Environ Sci Technol*, 2021.
- Ryder, O. S., Ault, A. P., Cahill, J. F., Guasco, T. L., Riedel, T. P., Cuadra-Rodriguez, L. A., Gaston, C. J., Fitzgerald, E., Lee, C., Prather, K. A., and Bertram, T. H.: On the Role of Particle Inorganic Mixing State in the Reactive Uptake of N<sub>2</sub>O<sub>5</sub> to Ambient Aerosol Particles, *Environmental Science & Technology*, 48, 1618-1627, 2014.
- Saiz-Lopez, A., and von Glasow, R.: Reactive halogen chemistry in the troposphere, *Chemical Society Reviews*, 41, 6448-6472, 2012.

- Sarwar, G., Simon, H., Xing, J., and Mathur, R.: Importance of tropospheric ClNO<sub>2</sub> chemistry across the Northern Hemisphere, *Geophysical Research Letters*, 41, 4050-4058, 2014.
- Seisel, S., Borensen, C., Vogt, R., and Zellner, R.: Kinetics and mechanism of the uptake of N<sub>2</sub>O<sub>5</sub> on mineral dust at 298 K, *Atmospheric Chemistry and Physics*, 5, 3423-3432, 2005.
- Simon, H., Kimura, Y., McGaughey, G., Allen, D. T., Brown, S. S., Osthoff, H. D., Roberts, J. M., Byun, D., and Lee, D.: Modeling the impact of ClNO<sub>2</sub> on ozone formation in the Houston area, *Journal of Geophysical Research-Atmospheres*, 114, 2009.
- Simpson, W. R., Brown, S. S., Saiz-Lopez, A., Thornton, J. A., and von Glasow, R.: Tropospheric Halogen Chemistry: Sources, Cycling, and Impacts, *Chemical Reviews*, 115, 4035-4062, 2015.
- Tang, M., Huang, X., Lu, K., Ge, M., Li, Y., Cheng, P., Zhu, T., Ding, A., Zhang, Y., Gligorovski, S., Song, W., Ding, X., Bi, X., and Wang, X.: Heterogeneous reactions of mineral dust aerosol: implications for tropospheric oxidation capacity, *Atmospheric Chemistry and Physics*, 17, 11727-11777, 2017.
- Tang, M., Zhang, H., Gu, W., Gao, J., Jian, X., Shi, G., Zhu, B., Xie, L., Guo, L., and Gao, X.: Hygroscopic properties of saline mineral dust from different regions in China: geographical variations, compositional dependence and atmospheric implications, *Journal of Geophysical Research: Atmospheres*, 124, 10844-10857, 2019.
- Tang, M. J., Thieser, J., Schuster, G., and Crowley, J. N.: Kinetics and mechanism of the heterogeneous reaction of N<sub>2</sub>O<sub>5</sub> with mineral dust particles, *Physical Chemistry Chemical Physics*, 14, 8551-8561, 2012.
- Thaler, R. D., Mielke, L. H., and Osthoff, H. D.: Quantification of Nitryl Chloride at Part Per Trillion Mixing Ratios by Thermal Dissociation Cavity Ring-Down Spectroscopy, *Analytical Chemistry*, 83, 2761-2766, 2011.
- Tham, Y. J., Yan, C., Xue, L., Zha, Q., Wang, X., and Wang, T.: Presence of high nitryl chloride in Asian coastal environment and its impact on atmospheric photochemistry, *Chinese Science Bulletin*, 59, 356-359, 2014.
- Tham, Y. J., Wang, Z., Li, Q., Yun, H., Wang, W., Wang, X., Xue, L., Lu, K., Ma, N., Bohn, B., Li, X., Kecorius, S., Groess, J., Shao, M., Wiedensohler, A., Zhang, Y., and Wang, T.: Significant concentrations of nitryl chloride sustained in the morning: investigations of the causes and impacts on ozone production in a polluted region of northern China, *Atmospheric Chemistry and Physics*, 16, 14959-14977, 2016.
- Tham, Y. J., Wang, Z., Li, Q., Wang, W., Wang, X., Lu, K., Ma, N., Yan, C., Kecorius, S., Wiedensohler, A., Zhang, Y., and Wang, T.: Heterogeneous N<sub>2</sub>O<sub>5</sub> uptake coefficient and production yield of ClNO<sub>2</sub> in polluted northern China: roles of aerosol water content and chemical composition, *Atmospheric Chemistry and Physics*, 18, 13155-13171, 2018.
- Thornton, J. A., Kercher, J. P., Riedel, T. P., Wagner, N. L., Cozic, J., Holloway, J. S., Dube, W. P., Wolfe, G. M., Quinn, P. K., Middlebrook, A. M., Alexander, B., and Brown, S. S.: A large atomic chlorine source inferred from mid-continental reactive nitrogen chemistry, *Nature*, 464, 271-274, 2010.
- Wang, H., Chen, J., and Lu, K.: Development of a portable cavity-enhanced absorption spectrometer for the measurement of ambient NO<sub>3</sub> and N<sub>2</sub>O<sub>5</sub>: experimental setup, lab characterizations, and field applications in a polluted urban environment, *Atmospheric Measurement Techniques*, 10, 1465, 2017a.
- Wang, H., Lu, K., Guo, S., Wu, Z., Shang, D., Tan, Z., Wang, Y., Le Breton, M., Lou, S., Tang, M., Wu, Y., Zhu, W., Zheng, J., Zeng, L., Hallquist, M., Hu, M., and Zhang, Y.: Efficient N<sub>2</sub>O<sub>5</sub>



- uptake and NO<sub>3</sub> oxidation in the outflow of urban Beijing, *Atmospheric Chemistry and Physics*, 18, 9705-9721, 2018.
- Wang, H., Tang, M., Tan, Z., Peng, C., and Lu, K.: Atmospheric Chemistry of Nitryl Chloride, *Progress in Chemistry*, 32, 1535-1546, 2020a.
- Wang, T., Tham, Y. J., Xue, L., Li, Q., Zha, Q., Wang, Z., Poon, S. C. N., Dube, W. P., Blake, D. R., Louie, P. K. K., Luk, C. W. Y., Tsui, W., and Brown, S. S.: Observations of nitryl chloride and modeling its source and effect on ozone in the planetary boundary layer of southern China, *Journal of Geophysical Research-Atmospheres*, 121, 2476-2489, 2016.
- Wang, X., Hua, T., Zhang, C., Lang, L., and Wang, H.: Aeolian salts in Gobi deserts of the western region of Inner Mongolia: Gone with the dust aerosols, *Atmospheric Research*, 118, 1-9, 2012.
- Wang, X., Wang, H., Xue, L., Wang, T., Wang, L., Gu, R., Wang, W., Tham, Y. J., Wang, Z., Yang, L., Chen, J., and Wang, W.: Observations of N<sub>2</sub>O<sub>5</sub> and ClNO<sub>2</sub> at a polluted urban surface site in North China: High N<sub>2</sub>O<sub>5</sub> uptake coefficients and low ClNO<sub>2</sub> product yields, *Atmospheric Environment*, 156, 125-134, 2017b.
- Wang, X., Jacob, D. J., Eastham, S. D., Sulprizio, M. P., Zhu, L., Chen, Q., Alexander, B., Sherwen, T., Evans, M. J., Lee, B. H., Haskins, J. D., Lopez-Hilfiker, F. D., Thornton, J. A., Huey, G. L., and Liao, H.: The role of chlorine in global tropospheric chemistry, *Atmospheric Chemistry and Physics*, 19, 3981-4003, 2019.
- Wang, X., Jacob, D. J., Fu, X., Wang, T., Le Breton, M., Hallquist, M., Liu, Z., McDuffie, E. E., and Liao, H.: Effects of Anthropogenic Chlorine on PM<sub>2.5</sub> and Ozone Air Quality in China, *Environmental Science & Technology*, 54, 9908-9916, 2020b.
- Wang, X., Jacob, D. J., Downs, W., Zhai, S., Zhu, L., Shah, V., Holmes, C. D., Sherwen, T., Alexander, B., Evans, M. J., Eastham, S. D., Neuman, J. A., Veres, P., Koenig, T. K., Volkamer, R., Huey, L. G., Bannan, T. J., Percival, C. J., Lee, B. H., and Thornton, J. A.: Global tropospheric halogen (Cl, Br, I) chemistry and its impact on oxidants, *Atmos. Chem. Phys. Discuss.*, 2021, 1-34, 2021.
- Wang, Z., Wang, W. H., Tham, Y. J., Li, Q. Y., Wang, H., Wen, L., Wang, X. F., and Wang, T.: Fast heterogeneous N<sub>2</sub>O<sub>5</sub> uptake and ClNO<sub>2</sub> production in power plant and industrial plumes observed in the nocturnal residual layer over the North China Plain, *Atmospheric Chemistry and Physics*, 17, 12361-12378, 2017c.
- Wu, C., Zhang, S., Wang, G., Lv, S., Li, D., Liu, L., Li, J., Liu, S., Du, W., Meng, J., Qiao, L., Zhou, M., Huang, C., and Wang, H.: Efficient Heterogeneous Formation of Ammonium Nitrate on the Saline Mineral Particle Surface in the Atmosphere of East Asia during Dust Storm Periods, *Environmental science & technology*, 54, 15622-15630, 2020.
- Young, C. J., Washenfelder, R. A., Edwards, P. M., Parrish, D. D., Gilman, J. B., Kuster, W. C., Mielke, L. H., Osthoff, H. D., Tsai, C., Pikelnaya, O., Stutz, J., Veres, P. R., Roberts, J. M., Griffith, S., Dusanter, S., Stevens, P. S., Flynn, J., Grossberg, N., Lefer, B., Holloway, J. S., Peischl, J., Ryerson, T. B., Atlas, E. L., Blake, D. R., and Brown, S. S.: Chlorine as a primary radical: evaluation of methods to understand its role in initiation of oxidative cycles, *Atmospheric Chemistry and Physics*, 14, 3427-3440, 2014.
- Yu, C., Wang, Z., Xia, M., Fu, X., Wang, W., Tham, Y. J., Chen, T., Zheng, P., Li, H., Shan, Y., Wang, X., Xue, L., Zhou, Y., Yue, D., Ou, Y., Gao, J., Lu, K., Brown, S. S., Zhang, Y., and Wang, T.: Heterogeneous N<sub>2</sub>O<sub>5</sub> reactions on atmospheric aerosols at four Chinese sites: improving model representation of uptake parameters, *Atmos. Chem. Phys.*, 20, 4367-4378, 2020.

- Zhang, H., Gu, W., Li, Y. J., and Tang, M.: Hygroscopic properties of sodium and potassium salts as related to saline mineral dusts and sea salt aerosols, *Journal of environmental sciences*, 95, 65-72, 2020.
- Zhang, X., Zhuang, G., Yuan, H., Rahn, K. A., Wang, Z., and An, Z.: Aerosol Particles from Dried Salt-Lakes and Saline Soils Carried on Dust Storms over Beijing, *Terrestrial Atmospheric and Oceanic Sciences*, 20, 619-628, 2009.
- Zhang, X. X., Sharratt, B., Liu, L. Y., Wang, Z. F., Pan, X. L., Lei, J. Q., Wu, S. X., Huang, S. Y., Guo, Y. H., Li, J., Tang, X., Yang, T., Tian, Y., Chen, X. S., Hao, J. Q., Zheng, H. T., Yang, Y. Y., and Lyu, Y. L.: East Asian dust storm in May 2017: observations, modelling, and its influence on the Asia-Pacific region, *Atmos. Chem. Phys.*, 18, 8353-8371, 2018.
- Zheng, B., Tong, D., Li, M., Liu, F., Hong, C., Geng, G., Li, H., Li, X., Peng, L., Qi, J., Yan, L., Zhang, Y., Zhao, H., Zheng, Y., He, K., and Zhang, Q.: Trends in China's anthropogenic emissions since 2010 as the consequence of clean air actions, *Atmospheric Chemistry and Physics*, 18, 14095-14111, 2018.

### Text S1. Parameterization for N<sub>2</sub>O<sub>5</sub> uptake on aqueous aerosols in GEOS-Chem

ClNO<sub>2</sub> can form from heterogeneous reaction of N<sub>2</sub>O<sub>5</sub> with Cl<sup>-</sup> on aqueous aerosols:



The rate reaction (R1) is determined by a reactive uptake coefficient,  $\gamma(\text{N}_2\text{O}_5)$ , representing the probability that a gas-phase N<sub>2</sub>O<sub>5</sub> molecule impacting the aerosol surface and to react in the bulk.

For aqueous aerosols, the model assumes that reaction (R1) happens on internally mixed sulfate, ammonium, nitrate, sea salt and organic aerosols, and account for the effect of organic coating as:

$$\frac{1}{\gamma_{\text{N}_2\text{O}_5}} = \frac{1}{\gamma_{\text{core}}} + \frac{1}{\gamma_{\text{coat}}} \quad (1)$$

where  $\gamma_{\text{core}}$  represents the reactive uptake mechanism of Bertram and Thornton (2009), and  $\gamma_{\text{coat}}$  represents the retardation from organic coating. Calculation of  $\gamma_{\text{coat}}$  is based on Riemer et al. (2009) with the relative humidity (RH) dependence of coating properties from Gaston et al. (2014). This parameterization has been described in detail by McDuffie et al. (2018a):

$$\gamma_{\text{N}_2\text{O}_5} = \frac{4V}{cS_a} H_{\text{aq}} k'_{2f} \left( 1 - \frac{1}{\left( \frac{k_3[\text{H}_2\text{O}]}{k_{2b}[\text{NO}_3^-]} \right) + 1 + \left( \frac{k_4[\text{Cl}^-]}{k_{2b}[\text{NO}_3^-]} \right)} \right) \quad (2)$$

$$k'_{2f} = \beta(1 - e^{-\delta[\text{H}_2\text{O}]}) \quad (3)$$

$$\gamma_{\text{coat}} = \frac{4RT H_{\text{org}} D_{\text{org}} R_c}{clR_p} \quad (4)$$

where  $R$  is the ideal gas constant,  $c$  is the gas-phase thermal velocity of N<sub>2</sub>O<sub>5</sub>,  $V$  and  $S_a$  are particle volume and surface area density,  $H_{\text{aq}}$  is Henry's law constant for N<sub>2</sub>O<sub>5</sub> in water;  $\beta$  is equal to  $1.15 \times 10^6 \text{ s}^{-1}$ ,  $\delta$  is equal to  $0.13 \text{ M}^{-1}$ ,  $k_3/k_{2b}$  is equal to 0.06,  $k_4/k_{2b}$  is equal to 29;  $H_{\text{org}} D_{\text{org}} = H_{\text{aq}} D_{\text{aq}}$  where  $D_{\text{aq}}$  is N<sub>2</sub>O<sub>5</sub> liquid diffusion coefficient, and  $\varepsilon$  is a scaling coefficient which increases linearly with the increase of RH;  $R_c$  and  $R_p$  are radius of inorganic core and the whole particle with organic coating, and  $l$  is the thickness of organic coating which is calculated using the volume ratio of organic and inorganic aerosols:

$$l = R_p(1 - \alpha^{\frac{1}{3}}) \quad (5)$$

$$\alpha = \frac{1}{1 + \frac{v_{organic}}{v_{inorganic}}} \quad (6)$$

The production yield of ClNO<sub>2</sub> in reaction (R1),  $\varphi$ , is calculated using the mechanism of Bertram and Thornton (2009) with a scaling factor of 0.25 following the suggestion by McDuffie et al. (2018b):

$$\varphi = 0.25 \left( \frac{k_2[\text{H}_2\text{O}]}{k_3[\text{Cl}^-]} + 1 \right)^{-1} \quad (7)$$

where  $k_3/k_2$  is equal to 450, as given by Roberts et al. (2009).

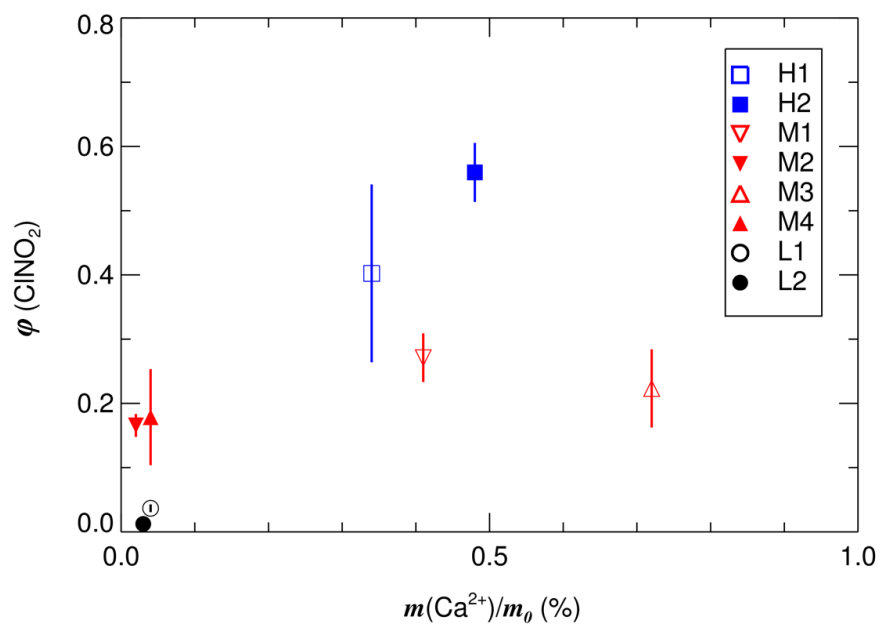


**Figure S1.** Measured  $\text{ClNO}_2$  yields at 18% RH versus mass fractions of soluble  $\text{Ca}^{2+}$  for the eight saline mineral dust samples.

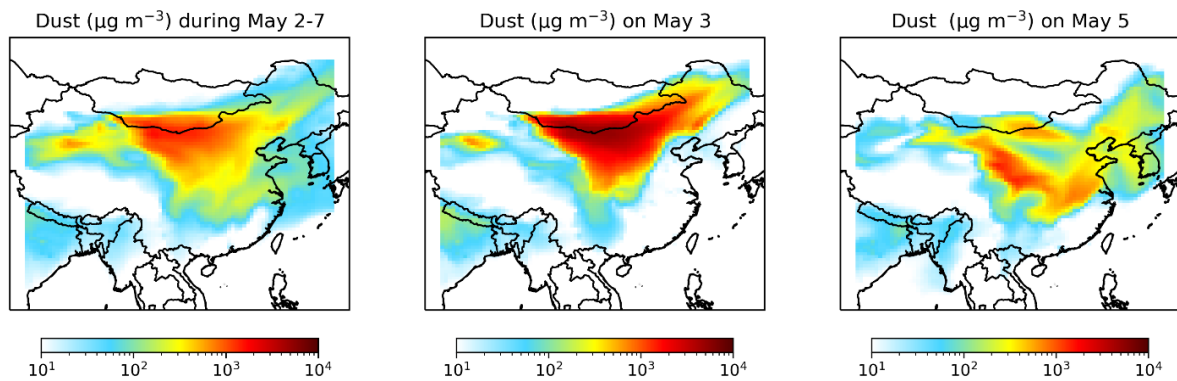


**Figure S2.** Modeled mean dust concentrations in the surface air over China during 2-7 May (left), on 3 May (middle) and on 5 May (right).

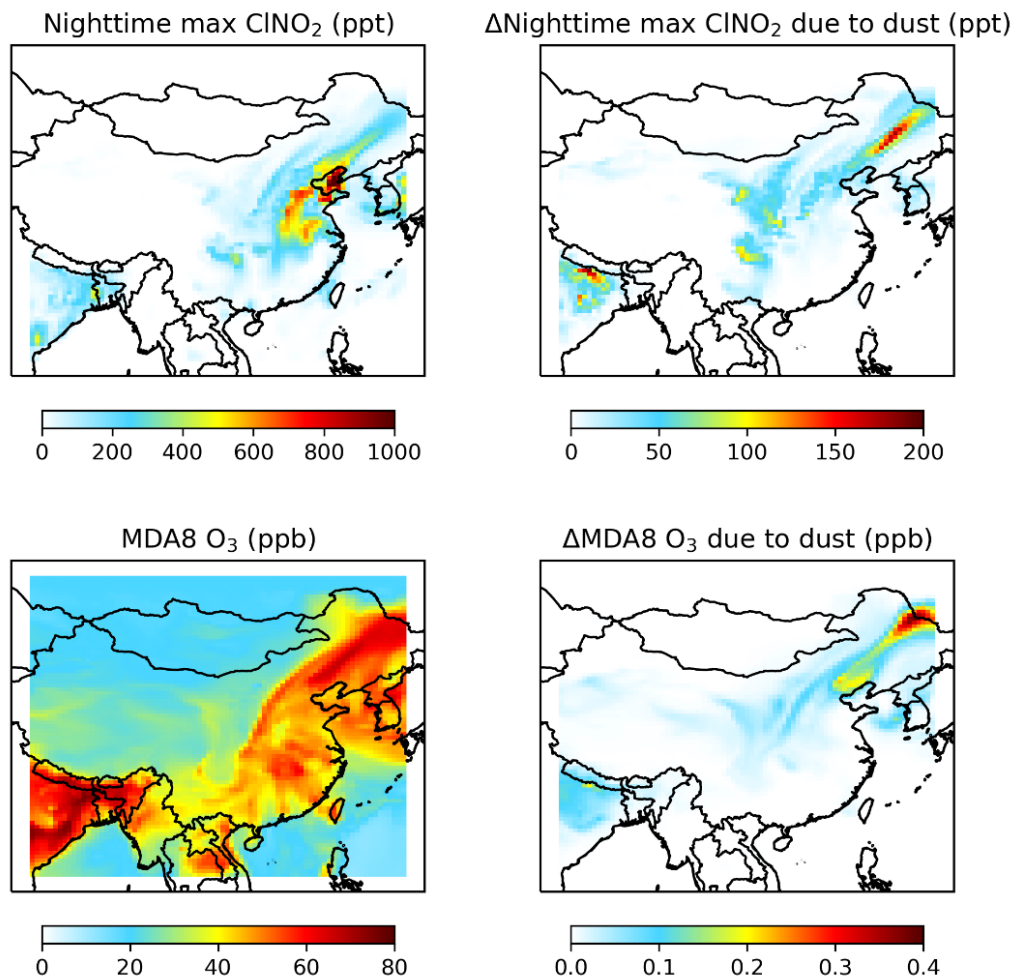


**Figure S3.** Modeled weekly mean mixing ratios of nighttime maximum  $\text{ClNO}_2$  (upper panels) and maximum daily 8-h average (MDA8) ozone (bottom panels) in surface air over China on 3 May 2017. The left panels show simulated mixing ratios in our standard case in which  $\phi(\text{ClNO}_2)$  is assumed to be 0 for  $\text{N}_2\text{O}_5$  uptake onto dust aerosol. The right panels show impacts of  $\text{ClNO}_2$  formation due to  $\text{N}_2\text{O}_5$  uptake onto dust, calculated as the difference between the standard case and the case in which  $\phi(\text{ClNO}_2)$  is assumed to be 0.1 for  $\text{N}_2\text{O}_5$  uptake onto dust.

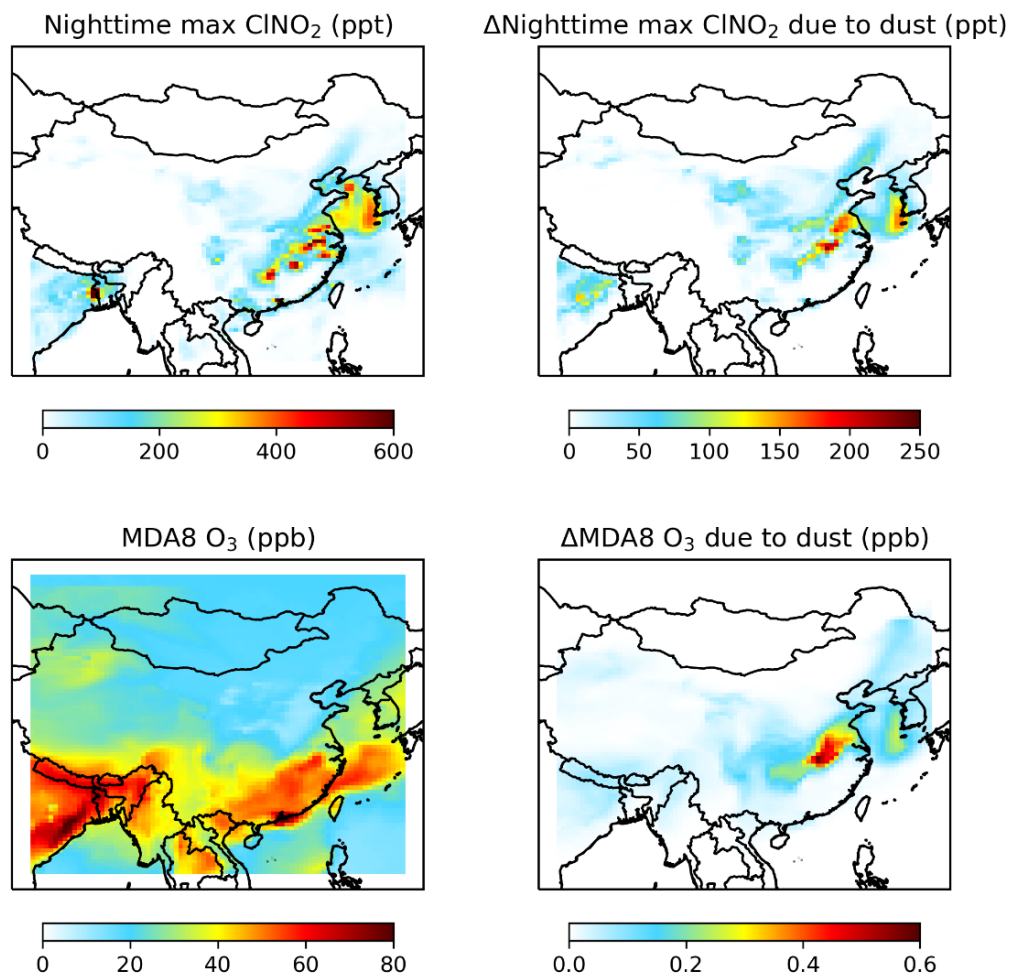


**Figure S4.** Same as Figure S3 but for 5 May 2017.



## References:

- Bertram, T. H. and Thornton, J. A.: Toward a general parameterization of N<sub>2</sub>O<sub>5</sub> reactivity on aqueous particles: the competing effects of particle liquid water, nitrate and chloride, *Atmos. Chem. Phys.*, 9, 8351-8363, 2009.
- Gaston, C. J., Thornton, J. A., and Ng, N. L.: Reactive uptake of N<sub>2</sub>O<sub>5</sub> to internally mixed inorganic and organic particles: the role of organic carbon oxidation state and inferred organic phase separations, *Atmos. Chem. Phys.*, 14, 5693-5707, 2014.
- McDuffie, E. E., Fibiger, D. L., Dube, W. P., Lopez-Hilfiker, F., Lee, B. H., Thornton, J. A., Shah, V., Jaegle, L., Guo, H. Y., Weber, R. J., Reeves, J. M., Weinheimer, A. J., Schroder, J. C., Campuzano-Jost, P., Jimenez, J. L., Dibb, J. E., Veres, P., Ebben, C., Sparks, T. L., Wooldridge, P. J., Cohen, R. C., Hornbrook, R. S., Apel, E. C., Campos, T., Hall, S. R., Ullmann, K., and Brown, S. S.: Heterogeneous N<sub>2</sub>O<sub>5</sub> Uptake During Winter: Aircraft Measurements During the 2015 WINTER Campaign and Critical Evaluation of Current Parameterizations, *J. Geophys. Res.-Atmos.*, 123, 4345-4372, 2018a.
- McDuffie, E. E., Fibiger, D. L., Dube, W. P., Hilfiker, F. L., Lee, B. H., Jaegle, L., Guo, H. Y., Weber, R. J., Reeves, J. M., Weinheimer, A. J., Schroder, J. C., Campuzano-Jost, P., Jimenez, J. L., Dibb, J. E., Veres, P., Ebben, C., Sparks, T. L., Wooldridge, P. J., Cohen, R. C., Campos, T., Hall, S. R., Ullmann, K., Roberts, J. M., Thornton, J. A., and Brown, S. S.: ClNO<sub>2</sub> Yields From Aircraft Measurements During the 2015 WINTER Campaign and Critical Evaluation of the Current Parameterization, *J. Geophys. Res.-Atmos.*, 123, 12994-13015, 2018b.
- Riener, N., Vogel, H., Vogel, B., Anttila, T., Kiendler-Scharr, A., and Mentel, T. F.: Relative importance of organic coatings for the heterogeneous hydrolysis of N<sub>2</sub>O<sub>5</sub> during summer in Europe, *J. Geophys. Res.-Atmos.*, 114, D17307, doi: 10.1029/2008jd011369, 2009.
- Roberts, J. M., Osthoff, H. D., Brown, S. S., Ravishankara, A. R., Coffman, D., Quinn, P., and Bates, T.: Laboratory studies of products of N<sub>2</sub>O<sub>5</sub> uptake on Cl<sup>-</sup> containing substrates, *Geophys. Res. Lett.*, 36, L20808, doi: 10.1029/2009GL040448, 2009.